EUR 3620 e

EUROPEAN ATOMIC ENERGY COMMUNITY - EURATOM

THE j_N METHOD FOR NEUTRON TRANSPORT PROBLEMS IN A HOMOGENEOUS SLAB

by

T. ASAOKA

1967

Joint Nuclear Research Center
Ispra Establishment - Italy

Reactor Physics Department
Reactor Theory and Analysis

LEGAL NOTICE

This document was prepared under the sponsorship of the Commission of the European Atomic Energy Community (EURATOM).

Neither the EURATOM Commission, its contractors nor any person acting on their behalf :

Make any warranty or representation, express or implied, with respect to the accuracy, completeness, or usefulness of the information contained in this document, or that the use of any information, apparatus, method, or process disclosed in this document may not infringe privately owned rights; or

Assume any liability with respect to the use of, or for damages resulting from the use of any information apparatus, method or process disclosed in this document.

This report is on sale at the addresses listed on cover page 4

at the price of FF 6.–	FB 60.–	DM 4.80	Lit. 750	Fl. 5.10

When ordering, please quote the EUR number and the title, which are indicated on the cover of each report.

Printed by SMEETS
Brussels, September 1967

EUR 3620 e

ERRATUM

THE j_N METHOD FOR NEUTRON TRANSPORT PROBLEMS IN A HOMOGENEOUS SLAB

by

T. ASAOKA

KEYWORDS

NEUTRONS
TRANSPORT THEORY
HOMOGENEOUS
CONFIGURATION
NUMERICALS
SCATTERING
ANGULAR DISTRIBUTION
GROUP THEORY
BUCKLING

Time dependence, accuracy, eigenvalues

EUR 3620 e

THE j_N METHOD FOR NEUTRON TRANSPORT PROBLEMS IN A HOMOGENEOUS SLAB by T. ASAOKA

European Atomic Energy Community - EURATOM
Joint Nuclear Research Center - Ispra Establishment (Italy)
Reactor Physics Department - Reactor Theory and Analysis
Brussels, September 1967 - 48 Pages - 15 Figures - FB 60

The j_N method (a new analytical approach) is applied within the context of a multigroup model to solve neutron transport problems for an infinite homogeneous slab with finite thickness under the assumption that the scattering of neutrons is spherically symmetric in the laboratory system.

Stationary energy-space-angle dependent problems are treated as a special case of time dependent problems. The numerical results for the

EUR 3620 e

THE j_N METHOD FOR NEUTRON TRANSPORT PROBLEMS IN A HOMOGENEOUS SLAB by T. ASAOKA

European Atomic Energy Community - EURATOM
Joint Nuclear Research Center - Ispra Establishment (Italy)
Reactor Physics Department - Reactor Theory and Analysis
Brussels, September 1967 - 48 Pages - 15 Figures - FB 60

The j_N method (a new analytical approach) is applied within the context of a multigroup model to solve neutron transport problems for an infinite homogeneous slah with finite thickness under the assumption that the scattering of neutrons is spherically symmetric in the laboratory system.

Stationary energy-space-angle dependent problems are treated as a special case of time dependent problems. The numerical results for the

vector flux generated by a stationary boundary source show that the j_5 approximation gives an accuracy comparable to the S_8 approximation in Carlson's theary, regardless of the size of the system.

The numerical values of the time-eigenvalues are shown for a one-group model and those of the first eigenvalue (asymptotic decay constant) are compared with Judge and Daitch's results. Their values agree well with the results of our j_0 approximation but appear slightly too large for thick slabs when compared to the more accurate j_4 results.

vector flux generated by a stationary boundary source show that the j_5 approximation gives an accuracy comparable to the S_8 approximation in Carlson's theary, regardless of the size of the system.

The numerical values of the time-eigenvalues are shown for a one-group model and those of the first eigenvalue (asymptotic decay constant) are compared with Judge and Daitch's results. Their values agree well with the results of our j_0 approximation but appear slightly too large for thick slabs when compared to the more accurate j_4 results.

EUR 3620 e

EUROPEAN ATOMIC ENERGY COMMUNITY - EURATOM

THE j_N METHOD FOR NEUTRON TRANSPORT PROBLEMS IN A HOMOGENEOUS SLAB

by

T. ASAOKA

1967

Joint Nuclear Research Center
Ispra Establishment - Italy

Reactor Physics Department
Reactor Theory and Analysis

SUMMARY

The j_N method (a new analytical approach) is applied within the context of a multigroup model to solve neutron transport problems for an infinite homogeneous slab with finite thickness under the assumption that the scattering of neutrons is spherically symmetric in the laboratory system.

Stationary energy-space-angle dependent problems are treated as a special case of time dependent problems. The numerical results for the vector flux generated by a stationary boundary source show that the j_5 approximation gives an accuracy comparable to the S_8 approximation in Carlson's theary, regardless of the size of the system.

The numerical values of the time-eigenvalues are shown for a one-group model and those of the first eigenvalue (asymptotic decay constant) are compared with Judge and Daitch's results. Their values agree well with the results of our j_0 approximation but appear slightly too large for thick slabs when compared to the more accurate j_4 results.

KEYWORDS

NEUTRONS
TRANSPORT THEORY
HOMOGENEOUS
CONFIGURATION
CORE
NUMERICALS
SCATTERING
TIME DEPENDENCE
ANGULAR DISTRIBUTION
ACCURACY
EIGENVALUES
GROUP THEORY
BUCKLUNG

CONTENTS

THE j_N METHOD FOR NEUTRON TRANSPORT PROBLEMS IN A HOMOGENEOUS SLAB (+)

1. Introduction

The j_N method is a new analytical approach which has emerged in the course of developing the multiple collision theory (Asaoka et al., 1964). The method is characterized by the introduction of a discontinuity factor into an integral equation govering the balance of neutrons (in contrast to the multiple collision method based on the neutron life-cycle viewpoint) to fix the point of measurement and by the use of expansions in spherical Bessel functions. When this expansion is truncated beyond the N-th order function, the resulting approximation has been called "the j_N approximation".

It has been shown in our latest publication (Asaoka, 1967) that the j_N method is a very useful tool for treating energy-space-time dependent transport problems in a bare spherical system. The stationary state can be treated as a limiting case of time-dependent problems and it is then easy to obtain the aymptotic time behaviour, critical condition or the value of the effective multiplication factor. For all these problems, the j_5 approximation has given results comparable in accuracy to the Carlson S_8 calculation.

The present work is concerned with a further development of the j_N method to deal with energy-space-angle-time dependent problems for an infinite homogeneous slab with finite thickness. (The results for stationary problems were partly submitted to the "Symposium on Advances in Reactor Theory", Karlsruhe, June 27-29, 1966 and some of the results for time-dependent problems were presented at the "International Conference on Research Reactor Utilization and Reactor Mathematics", Mexico City, May 2-4, 1967.)

(+) Manuscript received on July 21, 1967.

2. General Formulation for Time-Dependent Problems

We consider here, within the context of a multigroup (G energy-groups) model, an infinite homogeneous slab with finite thickness, a , in which the neutron scattering is spherically symmetric in the laboratory system.

Let x be the space co-ordinate, μ the direction cosine of the neutron velocity, Σ_g and v_g the macroscopic total cross-section and the speed of neutrons in the g-th energy-group respectively and $c(g'\to g)$ the mean number of secondary neutrons produced in the g-th group as a result of collisions in the g'-th group. Upon the surface at $x=0$, we assume a neutron source $S_g(\mu,t)\,d\mu\,dt$ for the g-th group incident with directions between μ and $\mu+d\mu$ $(\mu>0)$ during the time interval dt around time $t>0$.

The number of neutrons which, due to collisions in the g'-th group, are born in the g-th group with directions in the range $(\mu,\mu+d\mu)$, positions in the interval dx' around x' and at times in dt' around $t-t'$ is given by

$$\frac{c(g'\to g)}{2}\Sigma_{g'}\int_{-1}^{1}d\mu' v_{g'} n_{g'}(x',\mu',t-t')\,dx'dt'd\mu.$$

The probability that these neutrons travel for a time t' without further collision is $\exp(-\Sigma_g v_g t')$ and the space co-ordinate after this time is $x=x'+v_g\mu t'$. Hence, the number of the g-th group neutrons can be written as

$$\begin{aligned} n_g(x,\mu,t) = \sum_{g'=1}^{G}\int_0^t dt'\int_0^a dx'\int_{-1}^{1}d\mu'\,\frac{c(g'\to g)}{2}\Sigma_{g'}v_{g'}n_{g'}(x',\mu,t-t') \\ \times e^{-\Sigma_g v_g t'}\delta(x-x'-v_g\mu t') \\ +\int_0^t dt' S_g(\mu,t-t')e^{-\Sigma_g v_g t'}\delta(x-v_g\mu t')\Big]_{\mu>0}. \end{aligned} \tag{1}$$

Rewriting $\delta(x-x'-v_g\mu t')$ in the form of the Fourier representation

$$\frac{\Sigma_g}{2\pi}\int_{-\infty}^{\infty} dz\, \exp[i\Sigma_g z(x'+v_g\mu t'-x)],$$

equation (1) can be rewritten as follows:

$$v_g n_g(x,\mu,t) = \frac{v_g\Sigma_g}{2\pi}\int_{-\infty}^{\infty} dz \int_0^t dt' \int_0^a dx' \exp[i\Sigma_g z(x'+v_g\mu t'-x)]$$
$$\times \int_{-1}^{1} d\mu' \sum_{g'=1}^{G} \frac{c(g'\to g)}{2}\Sigma_{g'} v_{g'} n_{g'}(x',\mu',t-t') e^{-\Sigma_g v_g t'}$$
$$+ \frac{v_g\Sigma_g}{2\pi}\int_{-\infty}^{\infty} dz \int_0^t dt' \exp[i\Sigma_g z(v_g\mu t'-x)]\, S_g(\mu,t-t') e^{-\Sigma_g v_g t'}\Big]_{\mu>0}. \qquad (2)$$

The convolution integral in time on the right hand side suggests the application of the Laplace transform:

$$L_g(x,\mu,s) \equiv \int_0^{\infty} dt\, e^{-st}\, v_g n_g(x,\mu,t) e^{\Sigma_1 v_1 t}$$
$$= \frac{1}{2\pi}\int_0^a dx' \int_{-\infty}^{\infty} dz\, e^{i\Sigma_g z(x'-x)} \int_0^{\infty} dt' e^{-(P_g - iz\mu)t'} \sum_{g'=1}^{G} \int_{-1}^{1} d\mu' \frac{c(g'\to g)}{2}\Sigma_{g'} L_{g'}(x',\mu',s)$$
$$+ \frac{1}{2\pi}\int_{-\infty}^{\infty} dz\, e^{-i\Sigma_g z x} \int_0^{\infty} dt' e^{-(P_g - iz\mu)t'} L_{sg}(\mu,s)\Big]_{\mu>0},$$

(3)

where $P_g \equiv 1 - \frac{\Sigma_1 v_1 - s}{\Sigma_g v_g}$ and

$$L_{sg}(\mu,s) \equiv \int_0^{\infty} dt\, e^{-st} S_g(\mu,t) e^{\Sigma_1 v_1 t}.$$

Upon performing the integration over μ from -1 to 1, equation (3) gives:

$$L_g(x,s) \equiv \int_{-1}^{1} d\mu\, L_g(x,\mu,s)$$
$$= \frac{1}{2\pi}\int_{-\infty}^{\infty} \frac{dz}{z} e^{-i\Sigma_g z x} \int_0^{\infty} \frac{dt'}{t'} e^{-P_g t'} \sin(zt') \int_0^a dx' e^{i\Sigma_g z x'} \sum_{g'=1}^{G} c(g'\to g)\Sigma_{g'} L_{g'}(x',s)$$
$$+ \frac{1}{2\pi}\int_{-\infty}^{\infty} dz\, e^{-i\Sigma_g z x} \int_0^1 d\mu\, L_{sg}(\mu,s) \int_0^{\infty} dt' e^{-(P_g - iz\mu)t'}$$

(4)

From this equation together with the definition:

$$F(g'\to g, y, s) \equiv c(g'\to g)\Sigma_{g'}\int_0^a dx\, e^{i\Sigma_1(x-a/2)y} L_{g'}(x,s),$$

the following integral equation can be derived:

$$F(g\to g'', \tfrac{\Sigma_g}{\Sigma_1}y, s) = c(g\to g'')\Sigma_g a \frac{1}{2\pi}\int_{-\infty}^{\infty}\frac{dz}{z} j_0\left[\tfrac{\Sigma_g a}{2}(y-z)\right]\int_0^{\infty}\frac{dt'}{t'}e^{-P_g t'}\sin(zt')$$
$$\times \sum_{g'=1}^{G} F(g'\to g, \tfrac{\Sigma_g}{\Sigma_1}z, s)$$
$$+ c(g\to g'')\Sigma_g a\frac{1}{2\pi}\int_{-\infty}^{\infty}dz\, e^{-i\Sigma_g a z/2} j_0\left[\tfrac{\Sigma_g a}{2}(y-z)\right]\int_0^1 d\mu\, L_{sg}(\mu,s)\int_0^{\infty}dt'\, e^{-(P_g - iz\mu)t'},$$
(5)

where $j_n(z)$ is the n-th order spherical Bessel function.

Now, when we note that the symmetric kernel on the right hand side of equation (5) can be expanded by Gegenbauer's addition theorem, $j_0(y-z)=\sum_{p=0}^{\infty}(2p+1)j_p(y)j_p(z)$, we see that the function $F(g\to g'', y, s)$ can be expressed as a series in $j_m(\frac{\Sigma_1 a}{2}y)$:

$$F(g\to g'', y, s) = \sum_{m=0}^{\infty} b_m(g\to g'', s)\, j_m(\tfrac{\Sigma_1 a}{2}y).$$

Hence, equation (5) can be replaced by an equivalent system of linear equations governing the coefficients $b_m(g\to g'', s)$:

$$\frac{1}{2m+1} b_m(g\to g'', s) = c(g\to g'')\sum_{n=0}^{\infty} J_{mn}\left(\tfrac{\Sigma_g a}{2}, s\right)\sum_{g'=1}^{G} b_n(g'\to g, s)$$
$$+ c(g\to g'')\Sigma_g a\, S_g C_m\left(\tfrac{\Sigma_g a}{2}, s\right),$$
(6)

where

$$J_{mn}(\alpha_g, s) \equiv \frac{\alpha_g}{\pi}\int_{-\infty}^{\infty}\frac{dz}{z} j_m(\alpha_g z) j_n(\alpha_g z)\int_0^{\infty}\frac{dt'}{t'}e^{-P_g t'}\sin(zt'), \quad (7)$$

$$S_g C_m(\alpha_g, s) \equiv \frac{1}{2\pi}\int_{-\infty}^{\infty}dz\, e^{-i\alpha_g z} j_m(\alpha_g z)\int_0^1 d\mu\, L_{sg}(\mu, s)\int_0^{\infty}dt'\, e^{-(P_g - iz\mu)t'},$$
(8)

and use has been made of the orthogonality relation for spherical Bessel functions. When $s = \Sigma_1 v_1$ or $P_g = 1$, the integral $J_{mn}(\alpha_g, s)$ is reduced to $J(m,n)$ defined in a previous paper (Asaoka et al., 1964). An explicit expression for $J_{mn}(\alpha_g, s)$ has been given in appendix 1 of our latest paper (Asaoka, 1967).

It will be convenient to rewrite equation (6) here in terms of $B_m(g'', s) \equiv \sum_{g=1}^{G} b_m(g \to g'', s)$:

$$\frac{1}{2m+1} B_m(g'', s) = \sum_{g=1}^{G} c(g \to g'') \sum_{n=0}^{\infty} J_{mn}\left(\frac{\Sigma_g a}{2}, s\right) B_n(g, s) + \sum_{g=1}^{G} c(g \to g'') \Sigma_g a S_g C_m\left(\frac{\Sigma_g a}{2}, s\right). \tag{9}$$

Equation (3) can thus be written as follows:

$$L_g(x, \mu, s) = \sum_{m=0}^{\infty} B_m(g, s) F_m\left(\frac{\Sigma_g a}{2}, \frac{x}{a}, \mu, s\right) + \frac{1}{\mu} e^{-\Sigma_g x P_g/\mu} L_{sg}(\mu, s)\Big]_{\mu>0}, \tag{10}$$

where

$$F_m(\alpha_g, \xi, \mu, s) \equiv \frac{1}{4\pi} \int_{-\infty}^{\infty} dz\, e^{i\alpha_g z(1-2\xi)} j_m(\alpha_g z) \int_0^{\infty} dt'\, e^{-(P_g - iz\mu)t'}, \tag{11}$$

which is evaluated in Appendix 1.

Hence $n_g(x, \mu, t)$ can be transformed into the following form:

$$v_g n_g(x, \mu, t) = \frac{1}{2\pi i} \int_{\beta - i\infty}^{\beta + i\infty} ds\, e^{(s - \Sigma_1 v_1)t} L_g(x, \mu, s)$$
$$= \frac{1}{\mu} S_g\left(\mu, t - \frac{x}{v_g \mu}\right) e^{-\Sigma_g x/\mu}\Big]_{\mu>0} + \frac{1}{2\pi i} \int_{\beta - i\infty}^{\beta + i\infty} ds\, e^{(s - \Sigma_1 v_1)t} \sum_{m=0}^{\infty} B_m(g, s) \times F_m\left(\frac{\Sigma_g a}{2}, \frac{x}{a}, \mu, s\right). \tag{12}$$

As has been shown previously (Asaoka, 1967), the function $J_{00}(\alpha_g, s)$ is essentially singular when the real part of s is smaller than $\Sigma_1 v_1 - \Sigma_g v_g$ (the real part of P_g is negative) and hence so also is $B_m(g, s)$ The path of integration of the Laplace transform variable s on the right hand side of equation (12) is therefore to be deformed so that the real part of s is always larger than $\Sigma_1 v_1 - \Sigma_g v_g$ Thus we get:

$$v_g n_g(x,\mu,t) = \frac{1}{\mu} S_g(\mu, t-\frac{x}{v_g\mu}) e^{-\Sigma_g x/\mu} \Big]_{\mu>0}$$
$$+\sum_j \sum_{m=0}^{\infty} B_m(g,s_j) F_m(\frac{\Sigma_g a}{2}, \frac{x}{a}, \mu, \Sigma_1 v_1 s_j) e^{\Sigma_1 v_1 (s_j-1)t}$$
$$+\frac{1}{2\pi}\int_{-\infty}^{\infty} dy\, e^{-(\Sigma_g v_g - iy)t} \sum_{m=0}^{\infty} B_m(g, iy+\Sigma_1 v_1-\Sigma_g v_g) F_m(\frac{\Sigma_g a}{2}, \frac{x}{a}, \mu, iy+\Sigma_1 v_1-\Sigma_g v_g), \quad (13)$$

where $s=\Sigma_1 v_1 s_j$ (j = 1, 2, ...) is a pole of $B_m(g,s)$, $B_m(g,s_j)$ stands for the residue and the last term on the right hand side represents the contribution coming from the deformation of the integration path.

Upon integrating equation (13) over μ from - 1 to 1, the scalar flux is obtained in the form

$$v_g n_g(x,t) = \int_0^1 \frac{d\mu}{\mu} S_g(\mu, t-\frac{x}{v_g\mu}) e^{-\Sigma_g x/\mu}$$
$$+\sum_j \sum_{m=0}^{\infty} B_m(g,s_j) G_m(\frac{\Sigma_g a}{2}, \frac{2x}{a}-1, \Sigma_1 v_1 s_j) e^{\Sigma_1 v_1 (s_j-1)t}$$
$$+\frac{1}{2\pi}\int_{-\infty}^{\infty} dy\, e^{-(\Sigma_g v_g - iy)t} \sum_{m=0}^{\infty} B_m(g, iy+\Sigma_1 v_1-\Sigma_g v_g) G_m(\frac{\Sigma_g a}{2}, \frac{2x}{a}-1, iy+\Sigma_1 v_1-\Sigma_g v_g),$$

(14)

where

$$G_m(\alpha_g, \xi, s) \equiv \frac{1}{2\pi}\int_{-\infty}^{\infty} \frac{dz}{z} e^{-i\alpha_g \xi z} j_m(\alpha_g z) \int_0^{\infty} \frac{dt'}{t'} e^{-P_g t'} \sin(zt'). \quad (15)$$

The evalua ion of $G_m(\alpha_g, \xi, s)$ has been carried out in appendix 2 of a previous paper (Asaoka, 1967).

When we are interested in the number of leakage neutrons from the slab, it is only necessary to multiply equation (13) by $|\mu|$ and to fix the point of measurement at $x=x_0$ (x_0 = 0 to observe neutrons with $\mu<0$ reflected by the slab or $x_0=a$ for neutrons with $\mu>0$ transmitted through it). The total number of neutrons reflected by or transmitted through the slab is thus obtained by integrating $|\mu| v_g n_g(x_0,\mu,t)$

over μ from -1 to zero or from zero to 1. This gives

$$\int d\mu|\mu| v_g n_g(x_0,\mu,t) = \int_0^1 d\mu\, S_g(\mu, t-\frac{a}{v_g\mu}) e^{-\Sigma_g a/\mu}\Big]_{x_0=a}$$
$$+\sum_j \sum_{m=0}^{\infty} (2\frac{x_0}{a}-1)^m B_m(g,s_j) H_m(\frac{\Sigma_g a}{2}, \Sigma_1 v_1 s_j) e^{\Sigma_1 v_1(s_j-1)t}$$
$$+\frac{1}{2\pi}\int_{-\infty}^{\infty} dy\, e^{-(\Sigma_g v_g - iy)t} \sum_{m=0}^{\infty} (2\frac{x_0}{a}-1)^m B_m(g, iy+\Sigma_1 v_1 - \Sigma_g v_g) H_m(\frac{\Sigma_g a}{2}, iy+\Sigma_1 v_1-\Sigma_g v_g), \tag{16}$$

where
$$H_m(\alpha_g, s) \equiv \int_0^1 d\mu|\mu| F_m(\alpha_g, 1, |\mu|, s)$$
$$= \frac{1}{4\pi i}\int_{-\infty}^{\infty} \frac{dz}{z} e^{-i\alpha_g z} j_m(\alpha_g z) \int_0^{\infty} \frac{dt'}{t'} e^{-\beta_g t'} \left[(1+\frac{i}{zt'}) e^{izt'} - \frac{i}{zt'}\right]. \tag{17}$$

This expression for $H_m(\alpha_g, s)$ is evaluated in Appendix 2.

3. Formulae and Numerical Examples for Stationary Problems

From equation (13), (14) or (16), the asymptotic behaviour as $t\to\infty$ can be written as follows:

$$v_g n_g(x,\mu,t) \sim \frac{1}{\mu} S_g(\mu, t-\frac{x}{v_g\mu}) e^{-\Sigma_g x/\mu}\Big]_{\mu>0}$$
$$+\sum_{m=0}^{\infty} B_m(g,s_1) F_m(\frac{\Sigma_g a}{2}, \frac{x}{a}, \mu, \Sigma_1 v_1 s_1) e^{\Sigma_1 v_1(s_1-1)t}, \tag{18}$$

$$v_g n_g(x,t) \sim \int_0^1 \frac{d\mu}{\mu} S_g(\mu, t-\frac{x}{v_g\mu}) e^{-\Sigma_g x/\mu}$$
$$+\sum_{m=0}^{\infty} B_m(g,s_1) G_m(\frac{\Sigma_g a}{2}, \frac{2x}{a}-1, \Sigma_1 v_1 s_1) e^{\Sigma_1 v_1(s_1-1)t}, \tag{19}$$

$$\int d\mu |\mu| v_g n_g(x_0,\mu,t) \sim \int_0^1 d\mu S_g(\mu, t-\frac{a}{v_g\mu}) e^{-\Sigma_g a/\mu}]_{x_0=a} + \sum_{m=0}^{\infty} (2\frac{x_0}{a}-1)^m B_m(g, s_1) H_m(\frac{\Sigma_g a}{2}, \Sigma_1 v_1 s_1) e^{\Sigma_1 v_1 (s_1-1)t}, \tag{20}$$

where $s=\Sigma_1 v_1 s_1$ stands for the largest real pole of $B_m(g,s)$

When $S_g(\mu,t)\to 0$ as $t\to\infty$, the pole $\Sigma_1 v_1 s_1$ is to be obtained by solving the determinantal equation (see equation (9)):

$$\det \left| \frac{\delta_{gg'}\delta_{mn}}{2m+1} - c(g\to g') J_{mn}(\frac{\Sigma_g a}{2}, \Sigma_1 v_1 s_1) \right| = 0, \quad g, g'=1,2,\cdots,G \quad \text{for } m,n=0,2,4,\cdots, \tag{21}$$

where, contrary to the case of a spherically symmetric system treated in a previous paper (Asaoka, 1967), only the elements with even values for both m and n appear. This fact is due to certain symmetry relations holding for slab geometry, namely, $v_g n_g(x,\mu,t)=v_g n_g(a-x,-\mu,t)$ (see equation (11)), $v_g n_g(x,t)=v_g n_g(a-x,t)$ (see equation (15)) and $\int_{-1}^{0} d\mu|\mu| v_g n_g(0,\mu,t) = \int_0^1 d\mu |\mu| v_g n_g(a,\mu,t)$ (note that $j_m(-z)=(-1)^m j_m(z)$ and $J_{mn}(\alpha_g, s) = 0$ when $m+n$ = odd).

For a critical system, s_1 must be equal to unity and equation (21) with s_1 = 1 therefore gives the critical condition. This condition has already been worked out in some detail in a previous paper (Asaoka et al., 1964) for the special case of a one-group model. In order to obtain the value of the effective multiplication factor, k_{eff} , for a given reactor. $c(g\to g')$ is divided into two parts. These are the scattering part $c_s(g\to g')=\Sigma_s(g\to g')/\Sigma_g$ and the fission part $c_f(g\to g')$ $=\chi_{g'}(\nu\Sigma_f)_g/\Sigma_g$ where χ_g stands for the proportion of fission neutrons born in the g-th group ($\sum_{g=1}^{G}\chi_g$ = 1). Using this separation, the value of k_{eff} is obtained by solving equation (21) with s_1 = 1 and

$$c(g\to g') = c_s(g\to g') + c_f(g\to g')/k_{eff}.$$

The ratios between the residues $B_m(g, s_1)$ can now be determined by the use of equations (9) (with $\hat{S}_g = 0$) and (21) for any of the three above-mentioned problems, that is, the evaluation of the time-constant $s_1 - 1$, critical condition or k_{eff}. Having thus obtained the residues, the flux distribution can be obtained from equation (18), (19) or (20) with $S_g(\mu, t) = 0$ for each problem (these procedures are the same as for a spherical reactor described in a previous paper (Asaoka, 1967)).

For a subcritical system with a stationary boundary source $S_g(\mu)$ $(\mu > 0)$, only one pole $s = \Sigma_1 v_1$ of $B_m(g, s)$ is of importance. Hence, by multiplying $s - \Sigma_1 v_1$ on both sides of equation (9) and taking the limit $s \to \Sigma_1 v_1$, we get

$$\frac{1}{2m+1} B_m(g') = \sum_{g=1}^{G} c(g \to g') \sum_{n=0}^{\infty} J_{mn}\left(\frac{\Sigma_g a}{2}, \Sigma_1 v_1\right) B_n(g) + \sum_{g=1}^{G} c(g \to g') \Sigma_g a \hat{S}_g C_m\left(\frac{\Sigma_g a}{2}\right), \quad m = 0, 1, 2, \cdots, \tag{22}$$

where $B_m(g) \equiv \lim_{s \to \Sigma_1 v_1} (s - \Sigma_1 v_1) B_m(g, s)$ and (see equation (8))

$$\hat{S}_g C_m(\alpha_g) \equiv \lim_{s \to \Sigma_1 v_1} \hat{S}_g C_m(\alpha_g, s) = \frac{1}{2\pi} \int_{-\infty}^{\infty} dz\, e^{-i\alpha_g z} j_m(\alpha_g z) \int_0^1 d\mu \frac{S_g(\mu)}{1 - iz\mu}. \tag{23}$$

The stationary vector flux, scalar flux and the total number of leakage neutrons can thus be written as follows:

$$v_g n_g(x, \mu) = \frac{1}{\mu} S_g(\mu) e^{-\Sigma_g x/\mu} \Big]_{\mu > 0} + \sum_{m=0}^{\infty} B_m(g) F_m\left(\frac{\Sigma_g a}{2}, \frac{x}{a}, \mu, \Sigma_1 v_1\right), \tag{24}$$

$$v_g n_g(x) = \int_0^1 \frac{d\mu}{\mu} S_g(\mu) e^{-\Sigma_g x/\mu} + \sum_{m=0}^{\infty} B_m(g) G_m\left(\frac{\Sigma_g a}{2}, \frac{2x}{a} - 1, \Sigma_1 v_1\right), \tag{25}$$

$$\int d\mu |\mu| v_g n_g(x_0, \mu) = \int_0^1 d\mu\, S_g(\mu) e^{-\Sigma_g a/\mu} \Big]_{x_0 = a} + \sum_{m=0}^{\infty} \left(2\frac{x_0}{a} - 1\right)^m B_m(g) H_m\left(\frac{\Sigma_g a}{2}, \Sigma_1 v_1\right). \tag{26}$$

In addition, the expression for $|\mu| v_g n_g(x_0,\mu)$, the angular distribution of leakage neutrons, can be simplified to

$$|\mu| v_g n_g(x_0,\mu) = S_g(\mu) e^{-\Sigma_g a/\mu}\Big]_{x_0=a} + \frac{1}{2} \exp\left(-\frac{\Sigma_g a}{2|\mu|}\right) \sum_{m=0}^{\infty} B_m(g) j_m\left(-i\frac{\Sigma_g a}{2\mu}\right). \tag{27}$$

Equations (26) and (27) have been developed in a previous paper (Asaoka et al., 1964) for a one-group model and two cases where the angular distribution of the boundary source $S_g(\mu)$ is monodirectional or plane isotropic.

For the three cases where

(a) $S_g(\mu) = S_g$ (plane isotropic source),

(b) $S_g(\mu) = 2S_g\mu$ (point isotropic source),

(c) $S_g(\mu) = S_g\delta(\mu-\mu_1)$ with $\mu_1 > 0$ (monodirectional source),

the integral $C_m(\alpha_g)$ defined by equation (23) takes respectively the following forms (with $s = \Sigma_1 v_1$ and $P_g \equiv 1-(\Sigma_1 v_1 - s)/(\Sigma_g v_g)$):

$$C_m^a(\alpha_g, s) \equiv \frac{1}{2\pi i}\int_{-\infty}^{\infty} \frac{dz}{z} e^{-i\alpha_g z} j_m(\alpha_g z) \int_0^{\infty} \frac{dt'}{t'} e^{-P_g t'} (e^{izt'} - 1), \tag{28a}$$

$$C_m^b(\alpha_g, s) \equiv 4H_m(\alpha_g, s) \tag{28b}$$

$$C_m^c(\alpha_g, s) \equiv 2F_m(\alpha_g, 1, \mu_1, s)$$
$$\left(F_m(\alpha_g, 1, \mu_1, \Sigma_1 v_1) = \frac{1}{2\mu_1} j_m\left(-i\frac{\alpha_g}{\mu_1}\right) e^{-\alpha_g/\mu_1}\right), \tag{28c}$$

the explicit expression for $C_m^a(\alpha_g, s)$ being given in Appendix 3.

In order to give a numerical illustration of a multigroup model, calculations using 7 energy-groups were performed on water slabs (90% water in volume) of various thicknesses. A stationary point isotropic source with the spectrum given in Table 1 was assumed to exist on the plane

$x = 0$. In addition, a set of bucklings has been introduced to account for the finite extention of the water slab in other two directions, that is, in the y ($\sim$10 cm width) and z (24 cm height) directions. (The aim of this study was to determine the optimum moderator thickness for maximum thermal neutron leakage into the beam hole of the SORA reactor.) The buckling values are given in Table 1, together with the values of the macroscopic total and transport cross-sections (Σ_g and Σ_{trg}). The anisotropy of the neutron scattering is taken into account by using the transport approximation, that is, by the use of Σ_{trg} instead of Σ_g . In Table 2 are shown the numerical values of the mean number of secondary neutrons per collision:

$$c(g\rightarrow g')=\Sigma_s(g\rightarrow g')/[\Sigma_g+(B_y^2+B_z^2)_g/(3\Sigma_{trg})].$$

Figures 1, 2 and 3 show the spatial distributions of the total fluxes (scalar fluxes) in three slabs with thicknesses 1, 7 and 20 cm resp ectively. Each figure contains the results for the 3rd and 7th group flux. For comparison, the values in the S_4 and S_8 approximation (obtained by using the transport approximation and adopting the same values of $c(g\rightarrow g')$ as shown in Table 2) are also included in these figures. For thin slabs (see Fig. 1) the j_3 results agree quite well with those obtained from the S_8 calculation (only a slight underestimate is seen near the source boundary in the case of the 7th group). On the other hand, for thick slabs, the j_3 results deviate to some extent from the S_8 values in some places (see Fig. 3 where the S_4 calculation always gives slightly lower values than the S_8 results). It is seen, however, that the j_5 results are accurate enough to be comparable to those obtained from the S_4 or S_8 calculation.

Figures 4 and 5 show the angular distributions of the 3rd and 7th group neutron flux, respectively, in the slab with a thickness of 1 cm. In each figure, the angular distributions at three different places are shown, that is, at the source boundary ($x = 0$), in the middle of the slab ($x/a = 0.5$) and at the free boundary ($x/a = 1$). These were calculated by the use of the j_3 approximation and the values are normalized to unity at $\mu = 1$. As is seen in these figures, our results coincide nicely with those obtained from the S_8 calculation (the S_4 result for $\mu = 1/3$ at $x=a$ is slightly underestimated for the 7th group). The results for the slab with 7 cm thickness are shown in Figs. 6 and 7, where the difference between the j_3 and j_5 values is indistinguishable. At the source boundary where the angular distribution is discontinuous at $\mu = 0$ (the values for $\mu > 0$ are always equal to unity and represent the extraneous source), the results in the S_4 approximation deviate to some extent from ours (as do the S_8 results shown in Fig. 7). Figures 8 and 9 show the angular distributions in the slab with 20 cm thickness. The j_3 results around $\mu = 0$ (parallel direction to the slab boundary) differ appreciably from the j_5 values, especially at the free boundary where the values are discontinuous at $\mu = 0$ and always equal to zero for $\mu < 0$. It is seen, however, that the j_5 results are comparable in accuracy to those in the S_8 approximation, while the difference between the S_4 and S_8 results can be judged from the values at the source boundary shown in Fig. 9.

Figure 10 shows the vector fluxes of the 3rd, 6th and 7th group neutrons with the direction cosine $\mu = 1$ (outward normal direction) at the free boundary, i.e. curves of $v_g n_g(x=a, \mu=1)$ with $g = 3$, 6 or 7, as a function of slab thickness a. The difference between the j_3 and j_5 results is significant only for the 7th group neutrons in the very thick slabs.

Additional numerical calculations were performed on the water slab with a thickness of 7 cm by assuming a monodirectional source with $\mu_1 = 1$ and with the energy spectrum given in Table 1. The spatial distributions of the scalar fluxes for the 3rd, 6th and 7th group neutrons are shown in Fig. 11 (compare with Fig. 2) and the angular distributions of the 3rd and 7th group vector flux are given respectively in Figs. 12 and 13 (compare with Figs. 6 and 7 respectively).

4. Some Numerical Results for Time-Dependent Problems

For a homogeneous non-multiplying slab in which there is no up-scattering of neutrons, equation (9) can be reduced to

$$\left[\frac{1}{2m+1}-c(g\to g)J_{mm}\left(\frac{\Sigma_g a}{2},s\right)\right]B_m(g,s)$$
$$-c(g\to g)\sum_{\substack{n=0\\ n\neq m}}^{\infty} J_{mn}\left(\frac{\Sigma_g a}{2},s\right)B_n(g,s)$$
$$=\sum_{g'=1}^{g} S_{g'}c(g'\to g)\Sigma_{g'}aC_m\left(\frac{\Sigma_{g'}a}{2},s\right)+\sum_{g'=1}^{g-1}c(g'\to g)\sum_{n=0}^{\infty}J_{mn}\left(\frac{\Sigma_{g'}a}{2},s\right)B_n(g',s). \tag{29}$$

This equation indicates that the problem of finding the poles $s=\Sigma_1 v_1 s_j$ of $B_m(g,s)$ (see equation (13)) is the same as that in a one-group model:

$$\det\left|\frac{\delta_{mn}}{2m+1}-c(g\to g)J_{mn}\left(\frac{\Sigma_g a}{2},s\right)\right|=0, \tag{30}$$

where, in general, m and n take on all values, 0,1,2,.... (for a spherically symmetric system treated in a previous paper (Asaoka, 1967), they take on odd values only). Since $J_{mn}(\alpha_g,s)=0$ when $m+n$ = odd, this determinantal equation can be split into two equations; one contains only the elements with even values of m and n and the other contains only those with odd values of m and n. (In equation (13) or (14), the terms with even values of m on the right hand side are symmetric abount $x=a/2$ and $\mu=0$ and the others are antisymmetric, that is, $n_m(x,\mu,t)=(-1)^m n_m(a-x,-\mu,t)$ or $n_m(x,t)=(-1)^m n_m(a-x,t)$.) The equation with odd values is nothing more than the determinantal equation for a bare sphere with radius $\Sigma_g R=\Sigma_g a/2$ (see Asaoka, 1967). Hence, all poles which satisfy the condition $s_j>1-\Sigma_g v_g/(\Sigma_1 v_1)$ for a spherically symmetric system with radius $\Sigma_g R$ are, in general, also the poles for a slab with thickness $\Sigma_g a=2\Sigma_g R$ and with the same value of $c(g\to g)$.

The equation coming out of (30) on the basis of the elements with even values of m and n can be solved to find the poles by following the same procedure as illustrated for the spherically symmetric system since, in equation (30), $c(g\to g)$ is always contained in the form $P_g/c(g\to g)$ and $\Sigma_g a$ appears always in the form $\Sigma_g a P_g$ where $P_g \equiv 1-(\Sigma_1 v_1 - s)/(\Sigma_g v_g)$. Thus, the poles are located (as for the spherical system) as follows:

1) Draw the curves giving $1/c$ as a function of slab thickness Σa by solving equation (30) (with $s=\Sigma v$) in a one-group model. See Fig. 14(the smallest c gives the value required to keept a slab, of thickness Σa , critical)
2) Draw the diagonal of a rectangle with sides $1/c(g\to g)$ and $\Sigma_g a$ and find the abscissa $\Sigma_g a P_g$ of each point of intersection between the curves and the diagonal.

This shows that equation (30) with even values of m and n gives at most (N+2)/2 (and at least 1; see below) real poles for each energy-group, N being the order of the j_N approximation. (In addition to these poles, each g-th group has generally all poles of the higher g'-th groups which satisfy the condition $s_{jg'} > 1-\Sigma_1 v_1/(\Sigma_g v_g)$, because of the presence of the last term on the right hand side of equation (29).)

The asymptotic expressions for the poles P_g in the j_2 approximation are ($\alpha_g \equiv \Sigma_g a/2$, $c\alpha \equiv c(g\to g)\alpha_g$ and γ being the Euler Mascheroni constant):

$$\alpha_g P_g \sim \frac{1}{2}\exp\left[\frac{3}{2}-\gamma-\frac{1}{c\alpha}-\frac{1}{12}\frac{1}{1-12/(5c\alpha)}\right], \quad 0<\alpha_g P_g \ll 1, \tag{31}$$

$$\alpha_g P_g \sim c\alpha\left[1-\frac{5}{6(c\alpha)^2}\right] \text{ and } c\alpha\left[1-\frac{3}{2c\alpha}-\frac{17}{12(c\alpha)^2}\right], \quad \alpha_g P_g \gg 1. \tag{32}$$

Equation (31) shows that the asymptotic decay constant $\Sigma_1 v_1(1-s_1)$ (see equation (13) or (14)) tends to $\Sigma_g v_g$ as $c(g\to g)\Sigma_g a \to 0$, while equation (32) leads, for an infinite system, to the well known expression:

$$\Sigma_1 v_1 (1-s_j) \sim \Sigma_g v_g (1-c(g\to g)) = v_g\left[\Sigma_{ag} + \sum_{g'=g+1}^{G} \Sigma_s(g\to g')\right].$$

Table 3 shows the numerical values of the asymptotic decay constant, $1-s_1$ in a one-group model for infinite homogeneous slabs with various values of Σa and a fixed value of $C = 1$ (the value of s_1 for a slab with thickness $(\Sigma_a+\Sigma_s)a$ and with $C \neq 1$ is equal to the product of C and the s_1 corresponding to a system with $C = 1$ and a thickness $\Sigma a = \Sigma_s a = C(\Sigma_a+\Sigma_s)a$; this leads to the well known relation that the decay constant for the system with absorption is equal to the value for the system with purescattering plus $v\Sigma_a$). In Fig. 15, our results for the asymptotic decay constant are compared with those obtained from a variational calculation using a double-step spatial trial function (Judge and Daitch, 1964) and the experimentally observed values (Beghian and Wilensky, 1965). Our results in the j_0 approximation are on the curve showing Judge and Daitch's results. These values are slightly too large for slabs with large values of Σa compared to the more accurate results obtained from the j_4 approximation. The experimental results do not seem to be correct, especially for a thin slab, as Beghian and Wilensky have pointed out.

Table 4 shows the numerical values of the second time-eigenvalue, $1-s_3$ (the third eigenvalue for the system with the asymmetric components with odd values of m on the right hand side of equation (13) or (14)), obtained from equation (30) with even values of m and n and a one-group model which assumes a fixed value of $C = 1$. From equation (31), it is seen that, in the j_2 approximation, P_g takes the value zero also in the case where $C(g\to g)\Sigma_g a/2 = 12/5$ (corresponding to $1-s_3 = 1$ when $\Sigma a = 4.8$ in Table 4). In the j_4 approximation, the asymptotic expression for small $\alpha_g P_g > 0$ is obtained from:

$$\alpha_g P_g \sim \frac{1}{2}\exp\left[\frac{3}{2}-\gamma-\frac{1}{C\alpha}-\frac{1}{10}\,\frac{1-144/(35C\alpha)}{1-264/(35C\alpha)+576/(49(C\alpha)^2)}\right], \tag{31'}$$

which shows that $P_g = 0$ when $C\alpha = 0$ or $132(1\mp\sqrt{21/11})/35 = 2.200260$ ($1-s_3 = 1$ for $\Sigma a = 4.40052$ in Table 4) or 5.342597.

In Tables 5 and 6 are shown the numerical values of the second and fourth time-eigenvalues, $1-s_2$ and $1-s_4$ respectively, for a slab system with asymmetric flux components. These were obtained by solving equation (30) with odd values of m and n in a one-group model and represent respectively the asymptotic decay constant (the first eigenvalue) and the second eigenvalue for a bare sphere with radius $\Sigma R=\Sigma a/2$ and with c = 1 (see Asaoka, 1967). In the j_3 and j_5 approximation, the asymptotic expressions for the poles for small $|\alpha_g P_g|$ are respectively given by

$$\alpha_g P_g \sim \frac{35}{24}\left(1-\frac{18}{35}\left(5-\sqrt{\frac{19}{3}}\right)/(c\alpha)\right)\left(1-\frac{18}{35}\left(5+\sqrt{\frac{19}{3}}\right)/(c\alpha)\right)/\left(1-16/(5c\alpha)\right), \tag{33}$$

$$\begin{aligned}\alpha_g P_g &\sim \frac{5005}{3856}\,\frac{1-912/(77c\alpha)+2880/(77(c\alpha)^2)-115200/(3773(c\alpha)^3)}{1-15800/(1687c\alpha)+216000/(11809(c\alpha)^2)} \\ &= \frac{5005}{3856}\,\frac{(1-1.277148/(c\alpha))(1-3.281392/(c\alpha))(1-7.285614/(c\alpha))}{(1-2.775481/(c\alpha))(1-6.590257/(c\alpha))}\end{aligned} \tag{33'}$$

Equation (33) shows that P_g = 0 when $c\alpha=\frac{18}{35}\left(5\mp\sqrt{\frac{19}{3}}\right)$ (s_2= 0 for Σa = 2.554342$_5$ in Table 5 or s_4= 0 for Σa = 7.731372 in Table 6). On the other hand, the j_5 approximation gives the value P_g = 0 when $c\alpha$ = 1.277148 (Σa = 2.554296 in Table 5), 3.281392 (Σa = 6.562784 in Table 6) or 7.285614. In Tables 5 and 6, the negative values of s_2 and s_4 are not applicable for the present slab geometry.

5. Conclusion

The neutron transport problems for an infinite homogeneous slab with finite thickness dealt with in this report have been solved satisfactorily by the j_N method. In particular, it has been shown that for stationary energy-space-angle dependent problems the j_5 approximation which retains the first six terms of the expansions in spherical Bessel functions (the numerical treatment of these terms is the same as for the case where only three terms are retained) gives a result comparable in accuracy to the S_8 calculation for all systems studied.

A computer code for energy-space-angle-time dependent problems is now under preparation for the case where the boundary source is represented in a form of a delta function in time: $S_g(\mu,t)=S_g(\mu)\delta(t)$. In this case, $L_{sg}(\mu,s)=S_g(\mu)$ (see equation (3)) and the integral $C_m(\alpha_g,s)$ defined by equation (8) is reduced to the form given by equation (28a), (28b) or (28c) when the angular distribution of the source is plane isotropic, point isotropic or monodirectional.

In addition, the extention of the present method to solve multiregion problems is under way (the formulation for stationary one-group problems has been completed and the computer code is being written by Mrs. E. Caglioti of TCR, EURATOM-CCR, Ispra). Later, the j_N method will be adapted to treat also anisotropic scattering of neutrons.

References

Asaoka T. et al. (1964) J. Nuclear Energy, Parts A/B, 18, 665.

Asaoka T. (1967) "The j_N Method for Neutron Transport Problems in a Bare Sphere", to be published.

Beghian L.E., Wilensky S. (1965) Pulsed Neutron Research, 2, 511, IAEA, Vienna

Judge F.D., Daitch P.B. (1964) Nucl. Sci. Engng., 20, 428.

Appendix

1. Explicit expression for $F_m(\alpha_g,\xi,\mu,s)$ defined by equation (11)

Performing the integration over Z gives ($P_g \equiv 1-(\Sigma_1 v_1 - s)/(\Sigma_g v_g)$)

$$F_m(\alpha_g,\xi,\mu,s) \equiv \frac{1}{4\pi}\int_{-\infty}^{\infty} dZ\, e^{i\alpha_g Z(1-2\xi)}\, j_m(\alpha_g Z)\int_0^{\infty} dt'\, e^{-(P_g - iZ\mu)t'} \tag{11}$$

$$= \frac{i}{4\alpha_g}\int_0^{\infty} dt'\, e^{-P_g t'} \times \begin{cases} \mathrm{Res}\left[e^{i(1-2\xi+\frac{\mu t'}{\alpha_g})y}\left\{ j'_m(y)e^{iy} - (-1)^m j'_m(-y)e^{-iy}\right\}\right]_{y=0}, & t' < 2\alpha_g X/\mu, \\ S\,\mathrm{Res}\left[e^{i(1-2\xi+\mu t'/\alpha_g)y} j_m(y)\right]_{y=0}, & t' > 2\alpha_g X/\mu, \end{cases}$$

where

$$X \equiv \begin{cases} \xi \\ \xi - 1 \end{cases} \quad \text{and} \quad S \equiv \pm 1, \quad \text{when} \quad \mu \gtrless 0$$

and $\mathrm{Res}[f(y)]_{y=0}$ stands for the residue of $f(y)$ at $y = 0$ and $j_m(y)$ is split into two parts, $j_m(y) = j'_m(y)e^{iy} + (-1)^m j'_m(-y)e^{-iy}$, in which $j'_m(y)$ is a finite series in terms of negative powers of y. From the expression for $t' > 2\alpha_g X/\mu$, it is easily seen that the residue is always equal to zero when $t' > 2\alpha_g X/\mu$ because $j_m(y) \sim y^m/(2m+1)!!$ as $y \to 0$.

The explicit expression can thus be obtained in the following form by introducing the abbreviation $\alpha \equiv \alpha_g P_g$:

$$F_0 = \frac{1}{4\alpha}\left(1 - e^{-2\alpha X/\mu}\right),$$

$$F_1 = \frac{i}{4\alpha}\left[\frac{\mu}{\alpha} + 1 - 2\xi - S\left(\frac{|\mu|}{\alpha} + 1\right)e^{-2\alpha X/\mu}\right],$$

$$F_2 = -\frac{1}{4\alpha}\left[3\left(\frac{\mu}{\alpha}\right)^2 + 3(1-2\xi)\frac{\mu}{\alpha} + 1 - 6\xi(1-\xi) - \left(3\left(\frac{\mu}{\alpha}\right)^2 + 3\frac{|\mu|}{\alpha} + 1\right)e^{-2\alpha X/\mu}\right],$$

$$F_3 = -\frac{i}{4\alpha}\left[15\left(\frac{\mu}{\alpha}\right)^3 + 15(1-2\xi)\left(\frac{\mu}{\alpha}\right)^2 + 6(1-5\xi(1-\xi))\frac{\mu}{\alpha} + (1-2\xi)(1-10\xi(1-\xi)) - S\left(15\left(\frac{|\mu|}{\alpha}\right)^3 + 15\left(\frac{\mu}{\alpha}\right)^2 + 6\frac{|\mu|}{\alpha} + 1\right)e^{-2\alpha X/\mu}\right],$$

$$F_4=\frac{1}{4\alpha}\Big[105\left(\frac{\mu}{\alpha}\right)^4+105(1-2\xi)\left(\frac{\mu}{\alpha}\right)^3+45\left(1-\frac{14}{3}\xi(1-\xi)\right)\left(\frac{\mu}{\alpha}\right)^2$$
$$+10(1-2\xi)(1-7\xi(1-\xi))\frac{\mu}{\alpha}+1-20\xi(1-\xi)\left(1-\frac{7}{2}\xi(1-\xi)\right)$$
$$-\left(105\left(\frac{\mu}{\alpha}\right)^4+105\left(\frac{|\mu|}{\alpha}\right)^3+45\left(\frac{\mu}{\alpha}\right)^2+10\frac{|\mu|}{\alpha}+1\right)e^{-2\alpha x/\mu}\Big],$$

$$F_5=\frac{i}{4\alpha}\Big[945\left(\frac{\mu}{\alpha}\right)^5+945(1-2\xi)\left(\frac{\mu}{\alpha}\right)^4+420\left(1-\frac{9}{2}\xi(1-\xi)\right)\left(\frac{\mu}{\alpha}\right)^3$$
$$+105(1-2\xi)(1-6\xi(1-\xi))\left(\frac{\mu}{\alpha}\right)^2+15(1-14\xi(1-\xi)(1-3\xi(1-\xi)))\frac{\mu}{\alpha}$$
$$+(1-2\xi)\left(1-28\xi(1-\xi)\left(1-\frac{9}{2}\xi(1-\xi)\right)\right)$$
$$-S\left(945\left(\frac{|\mu|}{\alpha}\right)^5+945\left(\frac{\mu}{\alpha}\right)^4+420\left(\frac{|\mu|}{\alpha}\right)^3+105\left(\frac{\mu}{\alpha}\right)^2+15\frac{|\mu|}{\alpha}+1\right)e^{-2\alpha x/\mu}\Big],$$

$$F_6=-\frac{1}{4\alpha}\Big\{10395\left(\frac{\mu}{\alpha}\right)^6+10395(1-2\xi)\left(\frac{\mu}{\alpha}\right)^5+4725\left(1-\frac{22}{5}\xi(1-\xi)\right)\left(\frac{\mu}{\alpha}\right)^4$$
$$+1260(1-2\xi)\left(1-\frac{11}{2}\xi(1-\xi)\right)\left(\frac{\mu}{\alpha}\right)^3+210\left[1-12\xi(1-\xi)\left(1-\frac{11}{4}\xi(1-\xi)\right)\right]\left(\frac{\mu}{\alpha}\right)^2$$
$$+21(1-2\xi)\left[1-18\xi(1-\xi)\left(1-\frac{11}{3}\xi(1-\xi)\right)\right]\frac{\mu}{\alpha}$$
$$+1-42\xi(1-\xi)\left[1-9\xi(1-\xi)\left(1-\frac{22}{9}\xi(1-\xi)\right)\right]$$
$$-\Big[10395\left(\frac{\mu}{\alpha}\right)^6+10395\left(\frac{|\mu|}{\alpha}\right)^5+4725\left(\frac{\mu}{\alpha}\right)^4+1260\left(\frac{|\mu|}{\alpha}\right)^3+210\left(\frac{\mu}{\alpha}\right)^2$$
$$+21\frac{|\mu|}{\alpha}+1\Big]e^{-2\alpha x/\mu}\Big\},$$

$$F_7=-\frac{i}{4\alpha}\Big\{135135\left(\frac{\mu}{\alpha}\right)^7+135135(1-2\xi)\left(\frac{\mu}{\alpha}\right)^6+62370\left(1-\frac{13}{3}\xi(1-\xi)\right)\left(\frac{\mu}{\alpha}\right)^5$$
$$+17325(1-2\xi)\left(1-\frac{26}{5}\xi(1-\xi)\right)\left(\frac{\mu}{\alpha}\right)^4+3150\left[1-11\xi(1-\xi)\left(1-\frac{13}{5}\xi(1-\xi)\right)\right]\left(\frac{\mu}{\alpha}\right)^3$$
$$+378(1-2\xi)\left[1-\frac{44}{3}\xi(1-\xi)\left(1-\frac{13}{4}\xi(1-\xi)\right)\right]\left(\frac{\mu}{\alpha}\right)^2$$
$$+28\left[1-27\xi(1-\xi)\left(1-\frac{22}{3}\xi(1-\xi)\left(1-\frac{13}{6}\xi(1-\xi)\right)\right)\right]\frac{\mu}{\alpha}$$
$$+(1-2\xi)\left[1-54\xi(1-\xi)\left(1-11\xi(1-\xi)\left(1-\frac{26}{9}\xi(1-\xi)\right)\right)\right]$$
$$-S\Big[135135\left(\frac{|\mu|}{\alpha}\right)^7+135135\left(\frac{\mu}{\alpha}\right)^6+62370\left(\frac{|\mu|}{\alpha}\right)^5+17325\left(\frac{\mu}{\alpha}\right)^4$$
$$+3150\left(\frac{|\mu|}{\alpha}\right)^3+378\left(\frac{\mu}{\alpha}\right)^2+28\frac{|\mu|}{\alpha}+1\Big]e^{-2\alpha x/\mu}\Big\}$$

2. <u>Explicit expression for $H_m(\alpha_g, s)$ defined by equation (17)</u>

As in Appendix 1, the integration over z is first performed to give

$$H_m(\alpha_g, s) \equiv \frac{1}{4\pi i}\int_{-\infty}^{\infty}\frac{dz}{z}e^{-i\alpha_g z}j_m(\alpha_g z)\int_0^{\infty}\frac{dt'}{t'}e^{-P_g t'}\left[\left(1+\frac{i}{zt'}\right)e^{izt'}-\frac{i}{zt'}\right] \qquad (17)$$

$$= \frac{1}{4}\int_0^{\infty}\frac{dt'}{t'}e^{-P_g t'}\times\begin{cases} \mathrm{Res}\left[\frac{1}{y}\left\{j_m'(y)-(-1)^m j_m'(-y)e^{-2iy}\right\}\left\{\left(1+\frac{i\alpha_g}{yt'}\right)e^{it'y/\alpha_g}-\frac{i\alpha_g}{yt'}\right\}\right]_{y=0}, \\ \qquad t'<2\alpha_g, \\ \mathrm{Res}\left[\frac{1}{y}e^{-iy}j_m(y)\left\{\left(1+\frac{i\alpha_g}{yt'}\right)e^{it'y/\alpha_g}+\frac{i\alpha_g}{yt'}\right\}\right]_{y=0}, \quad t'>2\alpha_g. \end{cases}$$

This shows that when $t'>2\alpha_g$ the residue is equal to zero for all values of m except for $m = 0$ and 1. The explicit expression and the asymptotic formula for small $|\alpha|$ $(\alpha \equiv \alpha_g P_g)$ are thus obtained as follows (γ being the Euler-Mascheroni constant):

$$H_0 = \frac{1}{4}\left[\frac{1-e^{-2\alpha}}{2\alpha}+\int_1^{\infty}\frac{dy}{y^2}e^{-2\alpha y}\right] \sim \frac{1}{2}\left[1+\alpha\left(\gamma+\ln 2\alpha-\frac{3}{2}\right)-\sum_{p=2}^{\infty}\frac{(-2\alpha)^p}{(p-1)(p+1)!}\right],$$
$$\alpha>0,$$

$$H_1 = \frac{i}{4}\left[\frac{1-e^{-2\alpha}}{3\alpha^2}-\frac{3+e^{-2\alpha}}{6\alpha}+\frac{1}{3}\int_1^{y}\frac{dy}{y^2}e^{-2\alpha y}\right]$$
$$\sim \frac{i\alpha}{6}\left[\gamma+\ln 2\alpha-\frac{5}{6}-\alpha+\sum_{p=4}^{\infty}\frac{6(p-1)}{(p-2)(p+1)!}(-2\alpha)^{p-2}\right], \quad \alpha>0,$$

$$H_2 = -\frac{1}{8\alpha}\left[1-\frac{2+e^{-2\alpha}}{\alpha}+\frac{3}{2\alpha^2}(1-e^{-2\alpha})\right] \sim -\frac{\alpha}{24}\sum_{p=0}^{\infty}\frac{24(p+1)}{(p+4)!}(-2\alpha)^p,$$

$$H_3 = \frac{i}{8\alpha}\left[1-\frac{4-e^{-2\alpha}}{\alpha}+\frac{3(5+3e^{-2\alpha})}{2\alpha^2}-\frac{6(1-e^{-2\alpha})}{\alpha^3}\right] \sim i\frac{\alpha}{120}\left(1-\frac{2}{7}\alpha^2+\frac{4}{21}\alpha^3\right),$$

$$H_4 = \frac{1}{8\alpha}\left[1-\frac{20+3e^{-2\alpha}}{3\alpha}+\frac{45-17e^{-2\alpha}}{2\alpha^2}-\frac{14(3+2e^{-2\alpha})}{\alpha^3}+\frac{35(1-e^{-2\alpha})}{\alpha^4}\right]$$
$$\sim \frac{\alpha}{360}\left(1-\frac{4}{63}\alpha^3\right),$$

$$H_5 = -\frac{i}{8\alpha}\left[1-\frac{10-e^{-2\alpha}}{\alpha}+\frac{3(35+9e^{-2\alpha})}{2\alpha^2}-\frac{6(28-13e^{-2\alpha})}{\alpha^3}+\frac{45(7+5e^{-2\alpha})}{\alpha^4}\right.$$
$$\left.-\frac{270(1-e^{-2\alpha})}{\alpha^5}\right] \sim i\frac{\alpha}{840}\left(1+O(\alpha^4)\right).$$

3. <u>Explicit expression for $C_m^a(\alpha_g, s)$ defined by equation (28a)</u>

As in Appendix 1, performing the integration over z gives

$$C_m^a(\alpha_g, s) \equiv \frac{1}{2\pi i}\int_{-\infty}^{\infty}\frac{dz}{z}e^{-i\alpha_g z}j_m(\alpha_g z)\int_0^{\infty}\frac{dt'}{t'}e^{-P_g t'}(e^{izt'}-1) \tag{28a}$$

$$= \frac{1}{2}\int_0^{\infty}\frac{dt'}{t'}e^{-P_g t'} \times \begin{cases} \mathrm{Res}\left[\frac{1}{y}\left\{j_m'(y)-(-1)^m j_m'(-y)e^{-2iy}\right\}(e^{iyt'/\alpha_g}-1)\right]_{y=0}, & t'<2\alpha_g, \\ \mathrm{Res}\left[\frac{1}{y}e^{-iy}j_m(y)(e^{it'y/\alpha_g}+1)\right]_{y=0}, & t'>2\alpha_g. \end{cases}$$

This shows that when $t'>2\alpha_g$ the residue is equal to zero for all values of m except for $m = 0$. The explicit expression and the asymptotic formula for small $|\alpha|$ $(\alpha \equiv \alpha_g P_g)$ are obtained as follows:

$$C_0^a = \frac{1-e^{-2\alpha}}{2\alpha} + \int_1^{\infty}\frac{dy}{y}e^{-2\alpha y} \sim 1-\gamma-\ln 2\alpha - \sum_{p=1}^{\infty}\frac{(-2\alpha)^p}{p\cdot(p+1)!}\ , \quad \alpha>0,$$

$$C_1^a = -\frac{i}{2\alpha}\left(1-\frac{1-e^{-2\alpha}}{2\alpha}\right) \sim -\frac{i}{2}\sum_{p=2}^{\infty}\frac{2}{p!}(-2\alpha)^{p-2},$$

$$C_2^a = -\frac{1}{2\alpha}\left(1-\frac{3+e^{-2\alpha}}{2\alpha}+\frac{1-e^{-2\alpha}}{\alpha^2}\right) \sim -\frac{1}{6}\left(1-\frac{1}{5}\alpha^2+\frac{2}{15}\alpha^3-\frac{2}{35}\alpha^4\right),$$

$$C_3^a = \frac{i}{2\alpha}\left(1-\frac{6-e^{-2\alpha}}{2\alpha}+5\,\frac{2+e^{-2\alpha}}{2\alpha^2}-15\,\frac{1-e^{-2\alpha}}{4\alpha^3}\right) \sim \frac{i}{12}\left(1-\frac{4}{105}\alpha^3\right),$$

$$C_4^a = \frac{1}{2\alpha}\left(1-\frac{10+e^{-2\alpha}}{2\alpha}+3\,\frac{10-3e^{-2\alpha}}{2\alpha^2}-21\,\frac{5+3e^{-2\alpha}}{4\alpha^3}+21\,\frac{1-e^{-2\alpha}}{\alpha^4}\right) \sim \frac{1}{20}(1+O(\alpha^4)),$$

$$C_5^a = -\frac{i}{2\alpha}\left(1-\frac{15-e^{-2\alpha}}{2\alpha}+7\,\frac{5+e^{-2\alpha}}{\alpha^2}-21\,\frac{5-2e^{-2\alpha}}{\alpha^3}+63\,\frac{3+2e^{-2\alpha}}{\alpha^4}-315\,\frac{1-e^{-2\alpha}}{2\alpha^5}\right)$$

$$\sim -\frac{i}{30}(1+O(\alpha^4)).$$

Table 1 Boundary source spectrum, a set of buckling values and the nuclear cross-sections assumed for numerical calculations on water slabs (90% water in volume)

Energy-group			Source spectrum	Buckling	Σ_g	Σ_{trg}
g	Energy range	Average velocity	S_g (n/cm^2 sec)	$B_y^2 + B_z^2$ (cm^{-2})	(cm^{-1})	(cm^{-1})
1	10-3 MeV	2850 cm/μsec	0.001034	0.030	0.17543	0.07612
2	3-0.9	1712	0.004623	0.015	0.26738	0.11498
3	0.9-0.1	822.4	0.008280	0.005	0.57908	0.24900
4	100-3 keV	184.5	0.002594	0.015	1.14092	0.46778
5	3-0.0226	21.18	0.001174	0.030	1.61723	0.63086
6	22.3-0.414 eV	2.402	0.000492	0.045	1.71824	0.67124
7	0.414 eV-thermal	0.2881	0.000592	0.055	2.52418	1.65792

Table 2 Numerical values of the mean number of secondary neutrons per collision in water slabs

Energy-group g	$c(g \to g)$	$c(g \to g+1)$	$c(g \to g+2)$	$c(g \to g+3)$
1	0.23406	0.24752	0.07845	0.00785
2	0.38096	0.43149	0.04678	0.00089
3	0.67059	0.30788	0.01011	0
4	0.75139	0.23831	0.00102	0
5	0.86891	0.12040	0.00084	-
6	0.85253	0.13357	-	-
7	0.99011	-	-	-

Table 3 Asymptotic decay constants for infinite homogeneous slabs with $C = 1$ in a one-group model

Thickness Σa	Decay constant $1-s_1$	
	j_2 approx.	j_4 approx.
0.1	$^{*}5.1956_5\times10^{-8}$	$^{*}5.1957\times10^{-8}$
0.2	$^{*}5.7329\times10^{-4}$	$^{*}5.7330_5\times10^{-4}$
0.3	0.989255	0.989254_5
0.4	0.957051	0.957049_5
0.5	0.905493	0.905490
0.6	0.843992	0.843986
0.7	0.780147_5	0.780138_5
0.8	0.718366_5	0.718355
1.0	0.608089	0.608074
1.5	0.413221	0.413205
2.0	0.296855	0.296843
2.5	0.223383	0.223376
3.0	0.174267	0.174264
4.0	0.114716	0.114716
5.0	0.0813385	0.0813362
6.0	0.0607554	0.0607481
7.0	0.0471762	0.0471637
8.0	0.0377365	0.0377182
10.0	0.0258350	0.0258085
12.0	0.0183637_5	0.0183352
14.0	0.0145342	0.0144996
20.0	0.0080986	0.0080607

* values for s_1 ($s_1 = 0$ when $\Sigma a = 0$).

<u>Table 4</u> The second time-eigenvalue for a symmetric slab system (the third eigenvalue for an asymmetric slab system) with $C = 1$ in a one-group model

Thickness Σa	Time-eigenvalue $1-\lambda_3$	
	j_2 approx.	j_4 approx.
*	1	1
5	0.978187	0.837113
6	0.764917	0.606030
7	0.615101_5	0.459468_5
8	0.511749	0.361304
10	0.381296	0.241573
12	0.303363	0.173644_5
14	0.251846	0.131194
20	0.166989	0.068230

* Σa = 4.8 or 4.40052 in the j_2 or j_4 approximation

Table 5 The second time-eigenvalue for an asymmetric slab system with $c = 1$ in a one-group model

Thickness Σa	Time-eigenvalue $1-\lambda_2$	
	j_3 approx.	j_5 approx.
0.4	13.30210	13.30210
0.5	9.96427	9.96426
0.6	7.84035	7.84032
0.7	6.38405	6.38400
0.8	5.33123	5.33118
1.0	3.92531	3.92527
1.5	2.21107	2.21106
2.0	1.448733_5	1.448732
2.5	1.033564	1.033540
★	1	1
3.0	0.779077	0.779006
4.0	0.492604	0.492437
5.0	0.341557	0.341248
6.0	0.251515	0.251084
7.0	0.193338	0.192822
8.0	0.153442	0.152860
10.0	0.103652	0.102994
12.0	0.0748453	0.0741657
14.0	0.0566358	0.0559678
20.0	0.0294103	0.0288512

★ $\Sigma a = 2.55434$ or 2.55429_5 in the j_3 or j_5 approximation

Table 6 The fourth time-eigenvalue for an asymmetric slab system with $C = 1$ in a one-group model

Thickness Σa	Time-eigenvalue $1-s_4$	
	j_3 approx.	j_5 approx.
0.4	33.1759	32.3282
0.5	25.7336	25.1785_5
0.6	20.9003	20.5207
0.7	17.5248	17.2580_5
0.8	15.0429	14.8527
1.0	11.6538	11.5559
1.5	7.33428_5	7.32059_5
2.0	5.28879	5.28873
2.5	4.10833	4.09787
3.0	3.34237	3.30922
4.0	2.40237	2.29817
5.0	1.83332	1.63904
6.0	1.44066	1.18404
7.0	1.15669_5	0.884635_5
8.0	0.951168	0.686477
10.0	0.690369	0.451620
12.0	0.538589_5	0.322078
14.0	0.441105	0.242478
20.0	0.286313	0.126045

$s_4 = 0$ when $\Sigma a = 7.73137$ or 6.56278_5 in the j_3 or j_5 approximation.

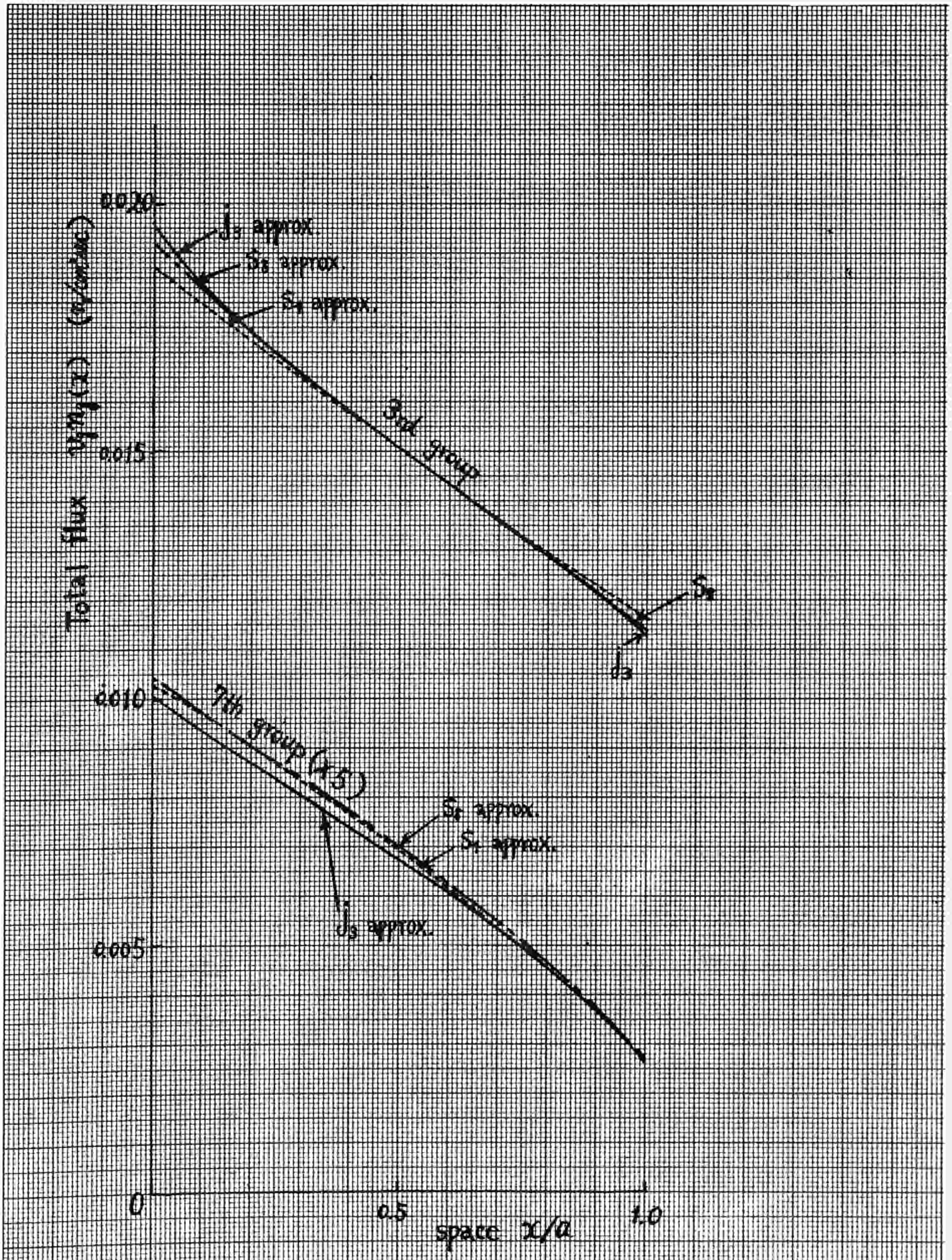

Fig. 1 – Stationary total flux distributions of the 3rd and 7th group neutrons in a water slab with thickness $a=1cm$

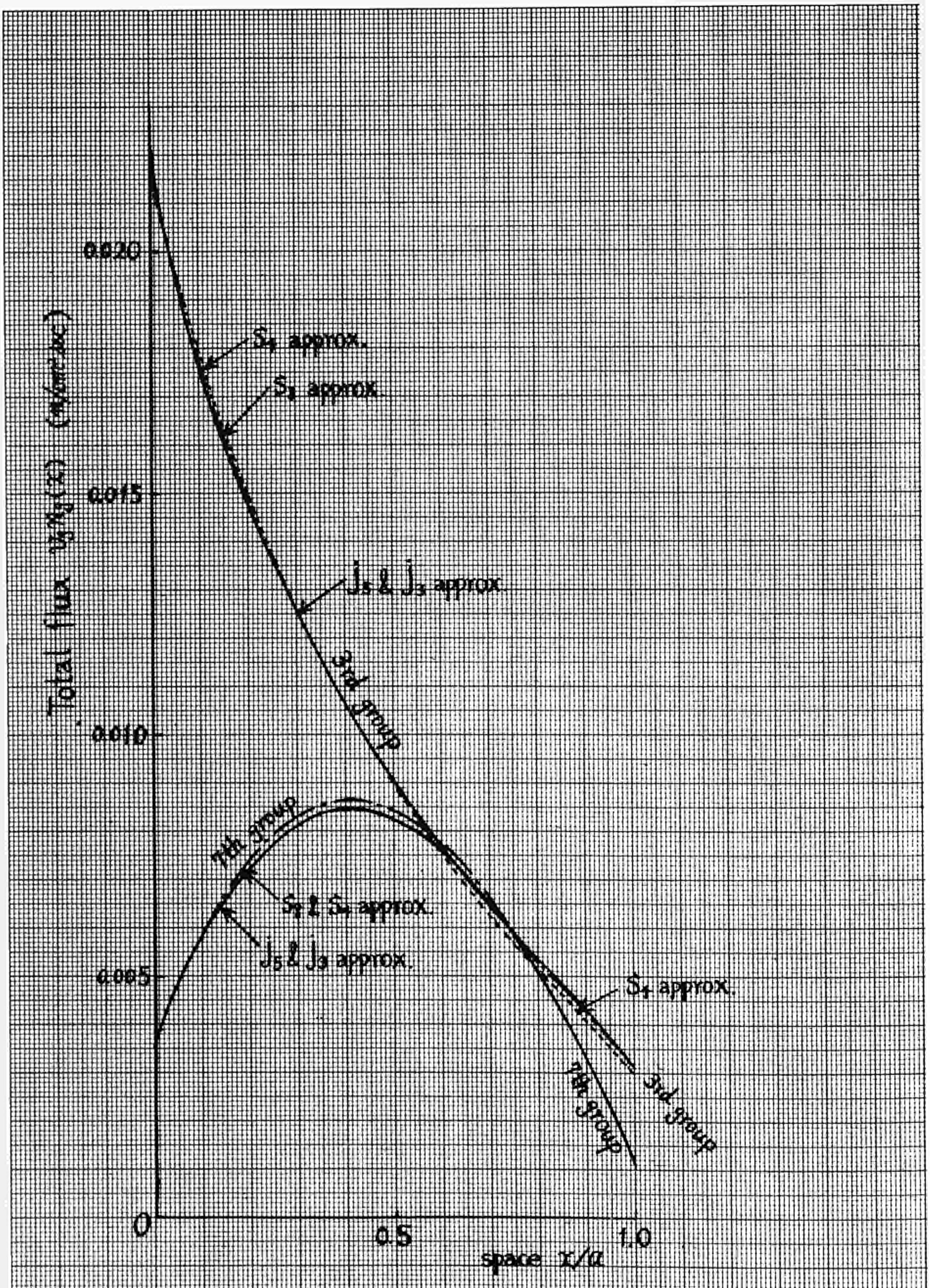

Fig. 2—Stationary total flux distributions of the 3rd and 7th group neutrons in a water slab with thickness $a=7cm$

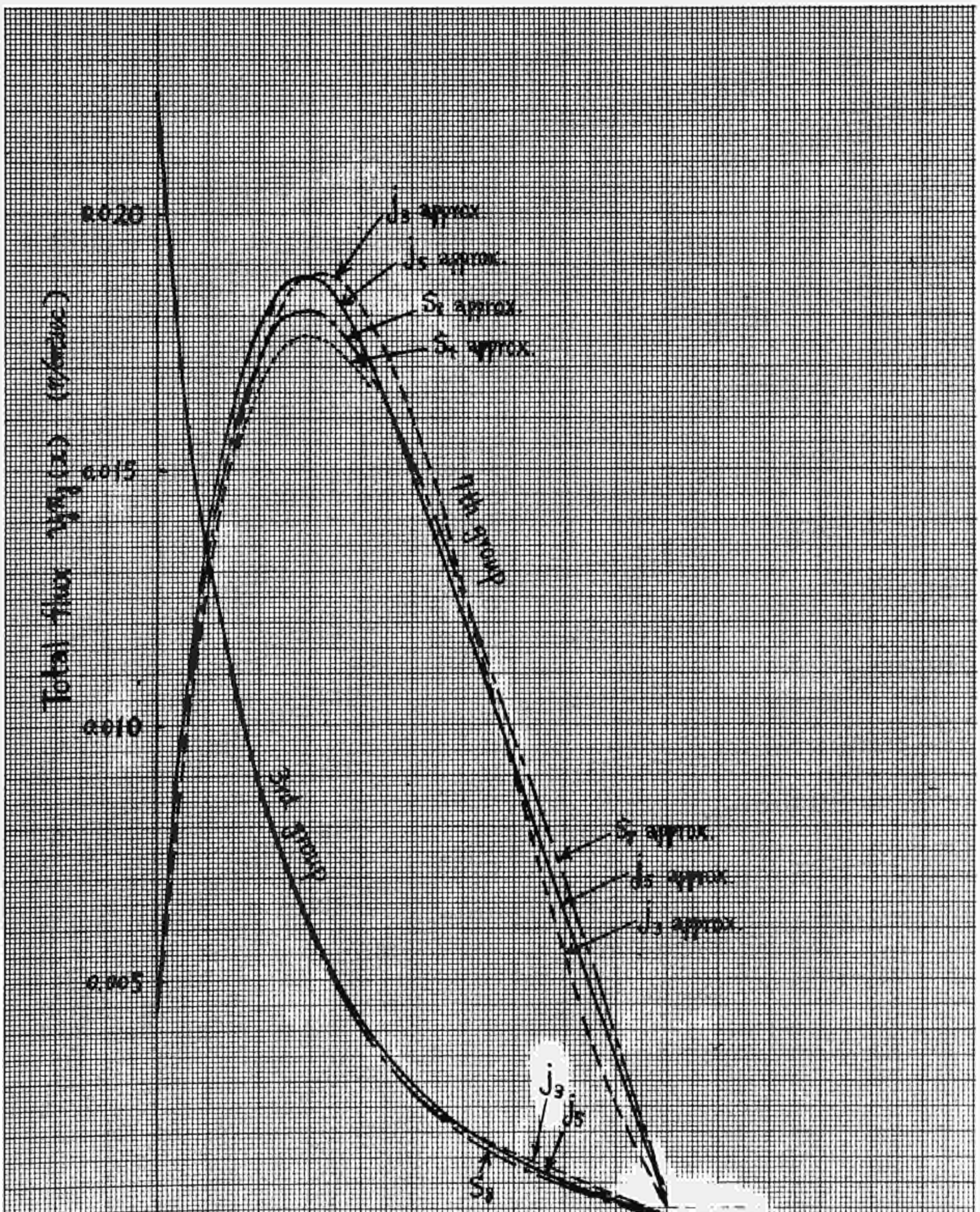

Fig. 3 - Stationary total flux distributions of the 3rd and 7th group neutrons in a water slab with thickness a=20 cm.

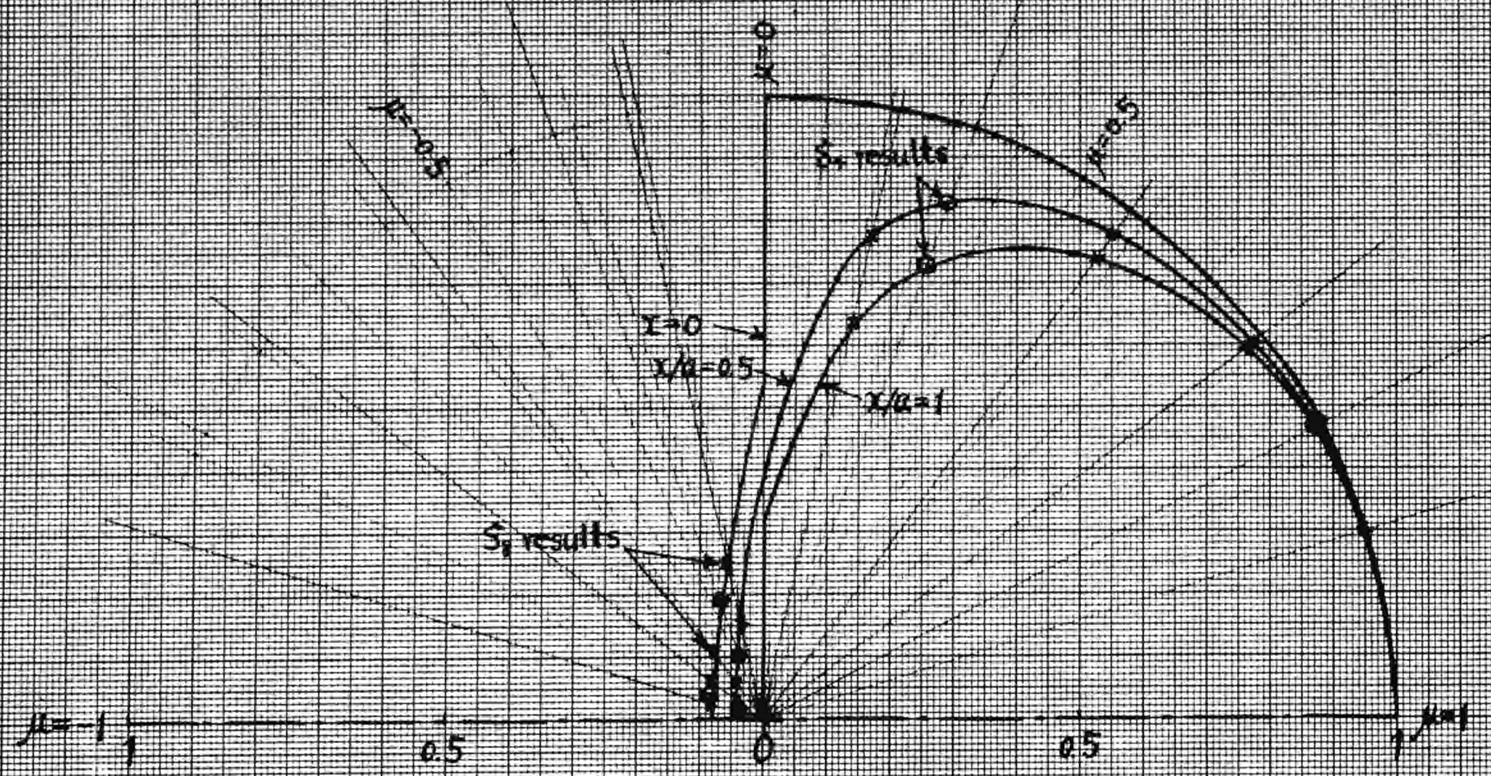

Fig. 4 — Stationary angular distributions of the 3rd group neutrons at 3 different places in a water slab with thickness $a=1$ cm (in the j_3 approximation)

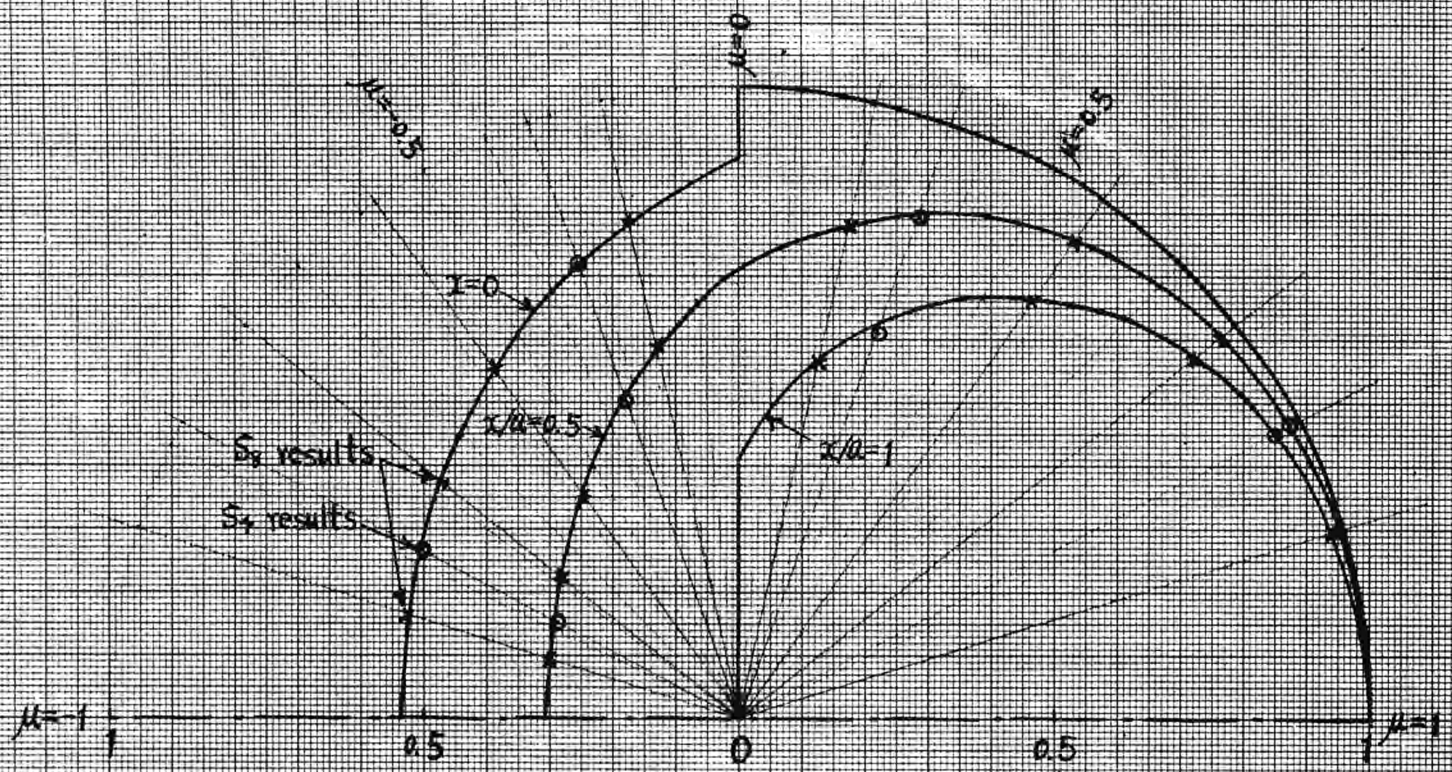

Fig. 5 – Stationary angular distributions of the 7th group neutrons at three different places in a water slab with thickness $a = 1\,cm$ (in the J_3 approximation)

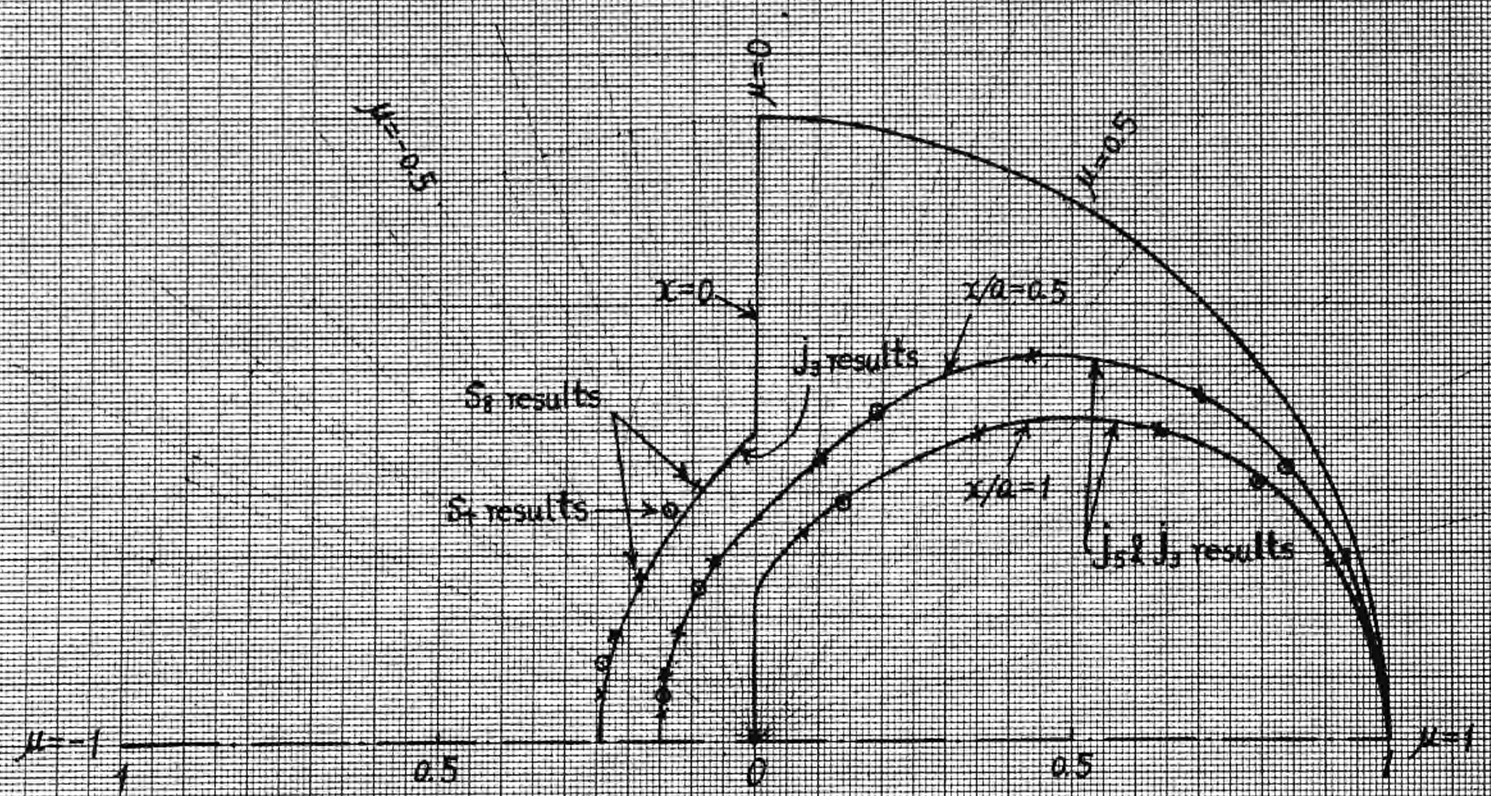

Fig. 6 – Stationary angular distributions of the 3rd group neutrons at 3 different places in a water slab with thickness $a=7\,cm$ (in the J_5 approximation)

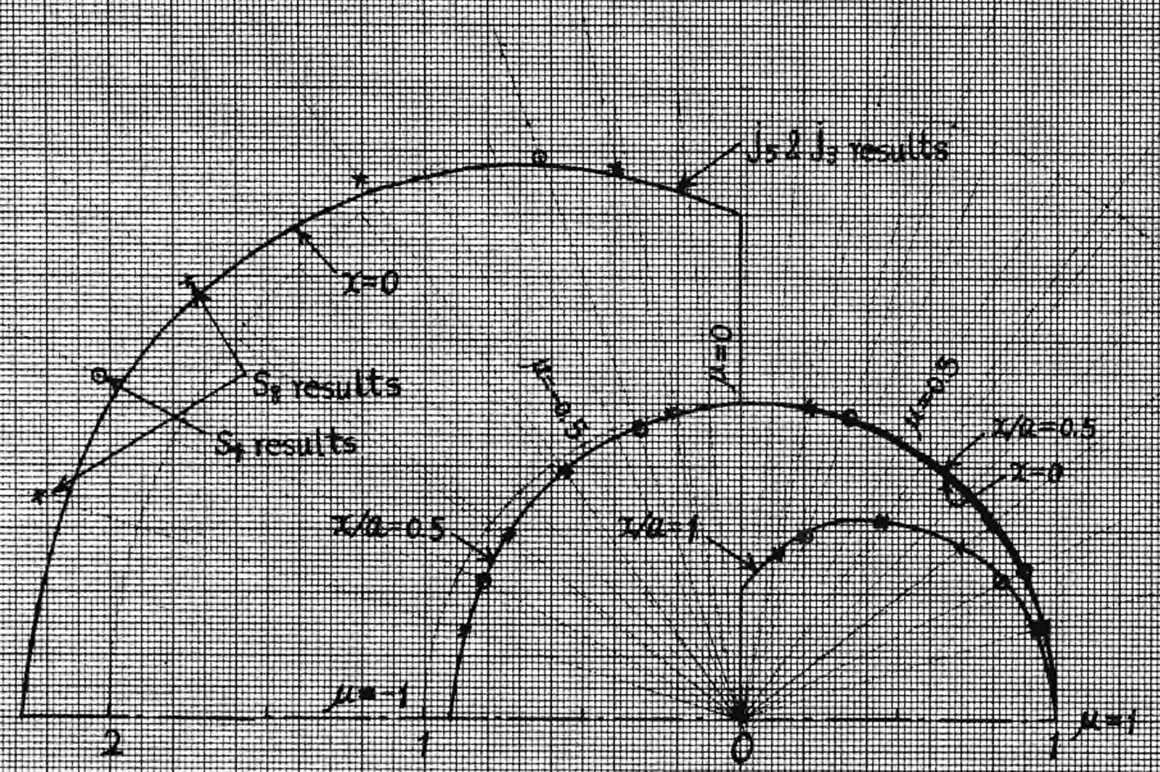

Fig.7 – Stationary angular distributions of the 7th group neutrons at 3 different places in a water slab with thickness $a=7cm$ (in the j_5 approximation)

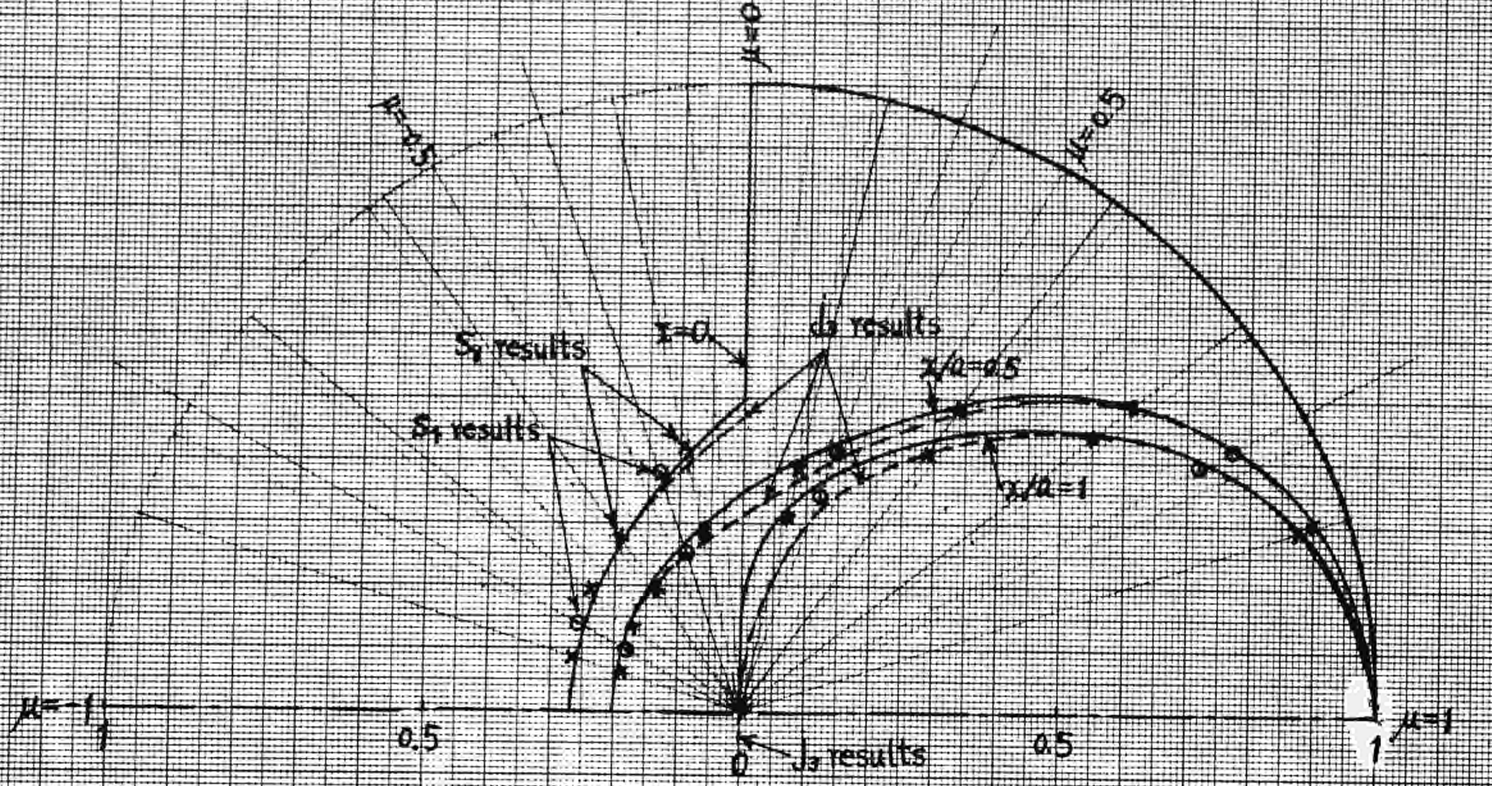

Fig. 8 — Stationary angular distributions of the 3rd group neutrons at 3 different places in a water slab with thickness $a = 20\,cm$ (in the j_5 approximation)

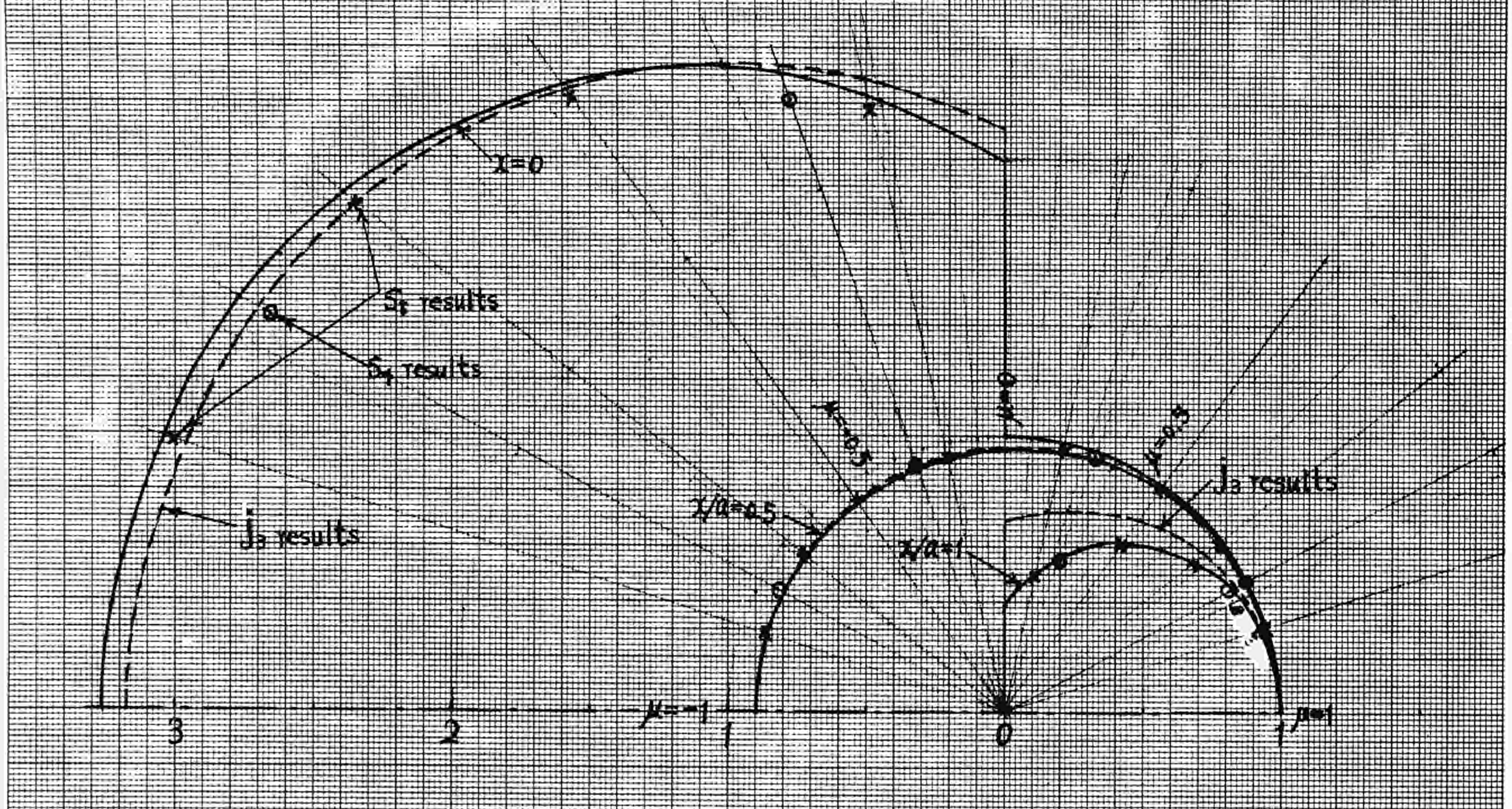

Fig. 9 — Stationary angular distribution of the 7th group neutrons at 3 different places in a water slab with thickness $a = 20\,cm$ (in the j_5 approximation)

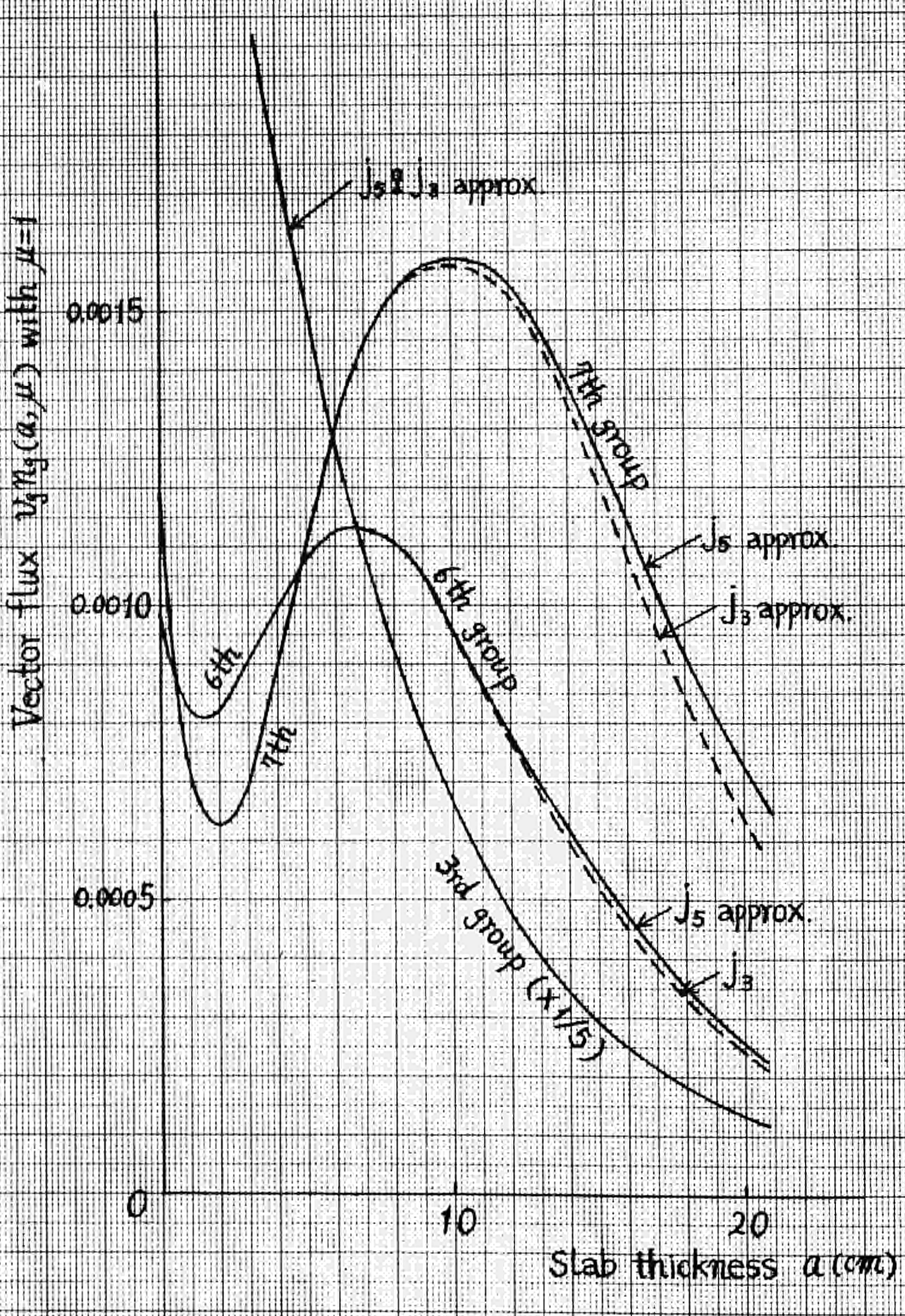

Fig. 10 – The vector fluxes of the 3rd, 6th and 7th group neutrons with $\mu=1$ at the free boundary of water slabs with various thicknesses

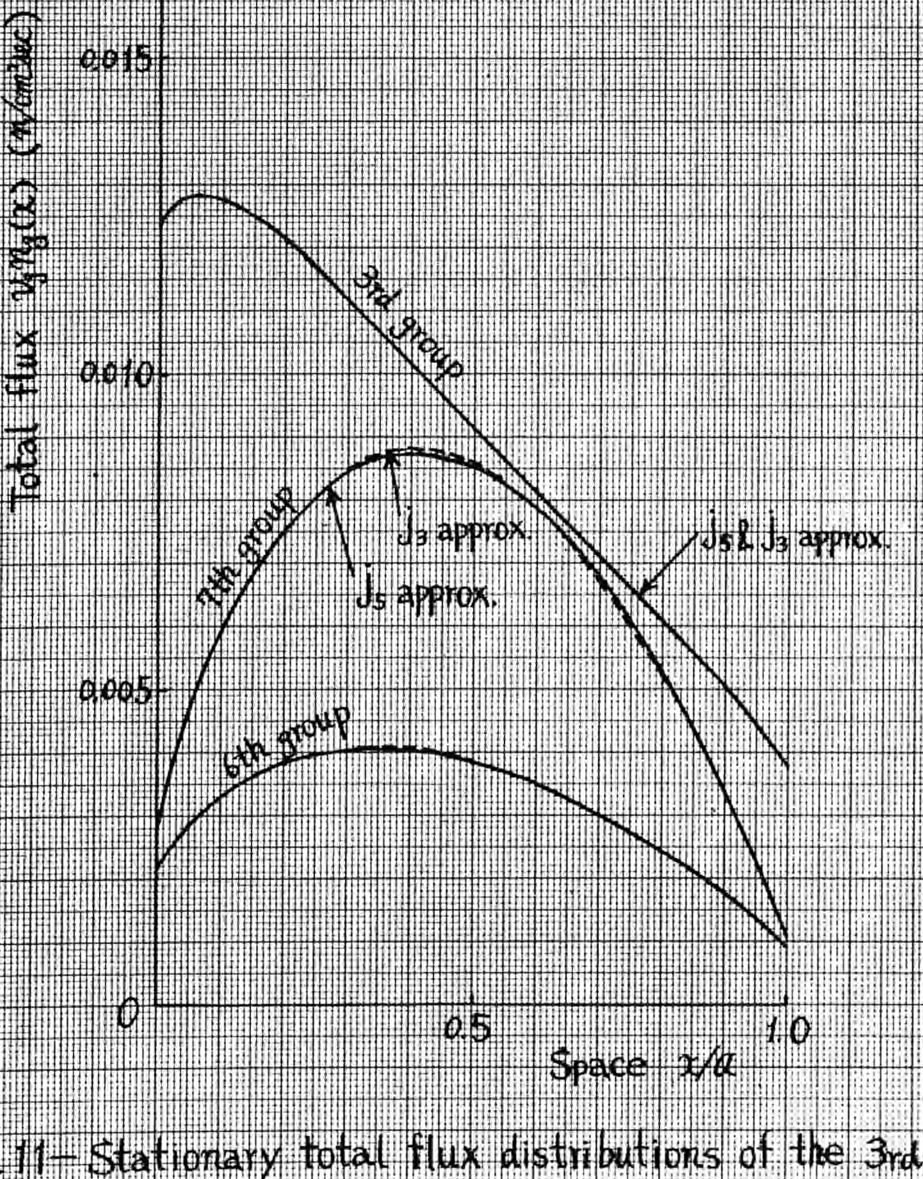

Fig. 11– Stationary total flux distributions of the 3rd, 6th and 7th group neutrons in a water slab with 7 cm thickness due to a monodirectional boundary source

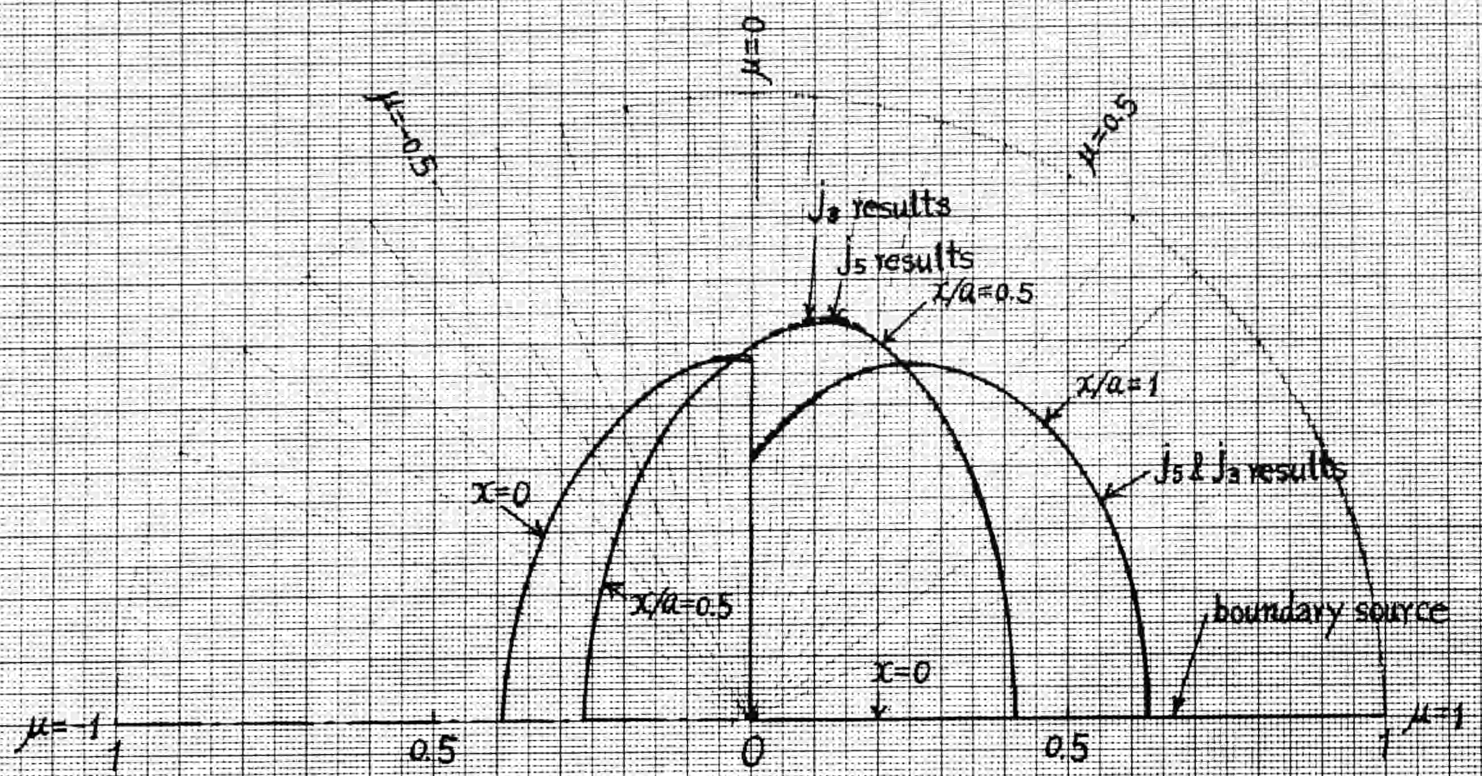

Fig. 12– Angular distributions of the 3rd group neutrons at 3 different places in a water slab with 7 cm thickness due to a monodirectional boundary source

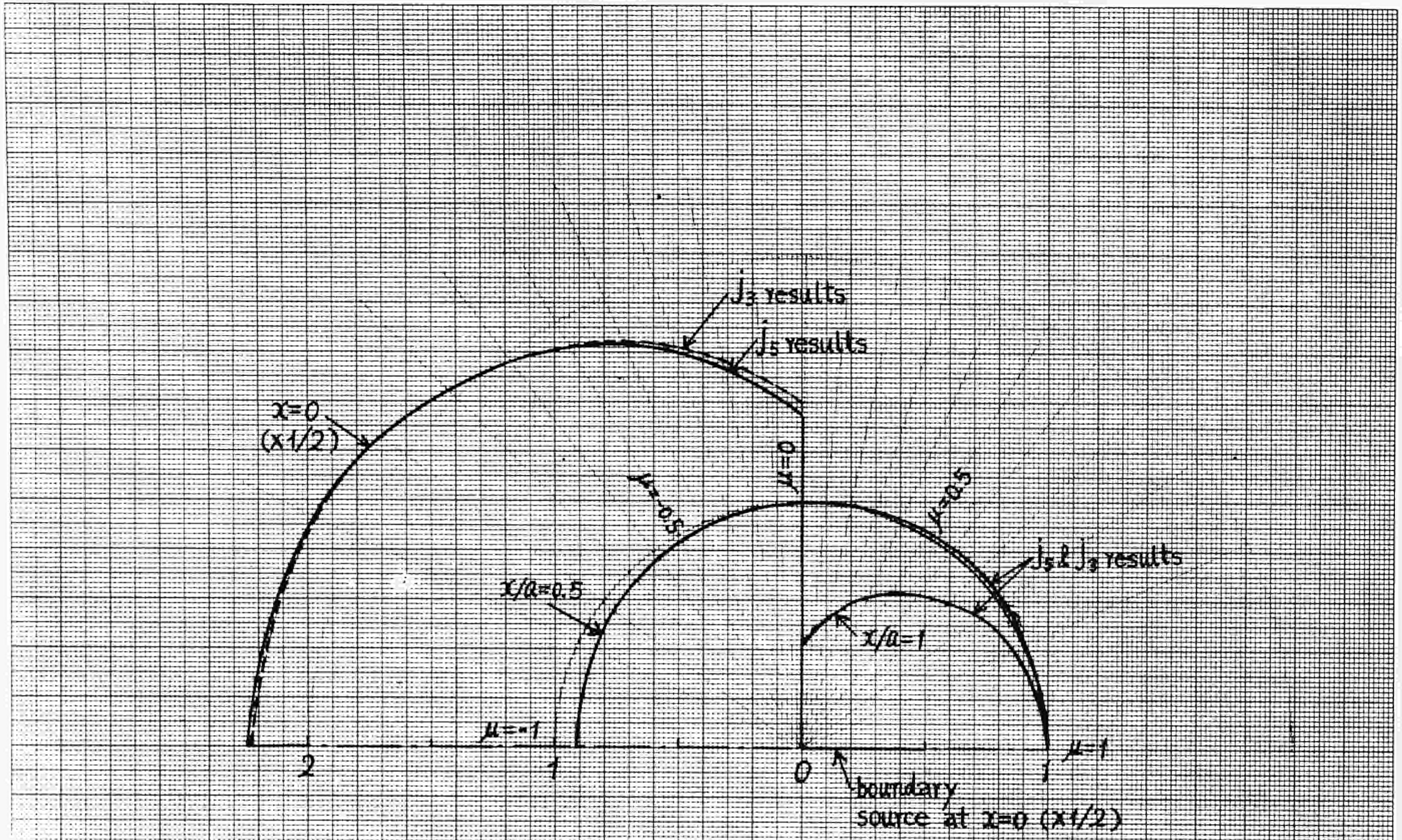

Fig. 13—Angular distributions of the 7th group neutrons at 3 different places in a water slab with 7 cm thickness due to a monodirectional boundary source

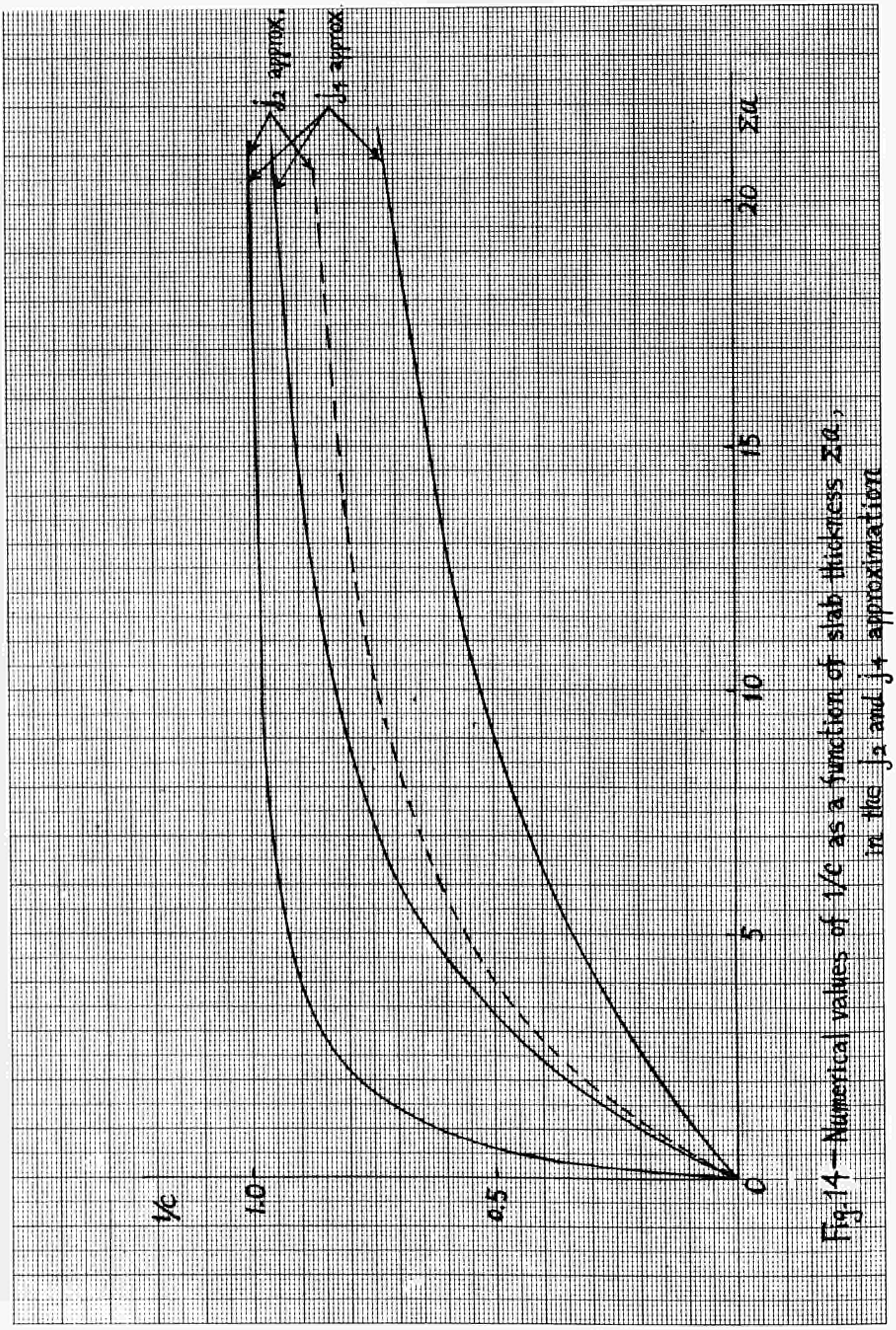

Fig. 14 — Numerical values of 1/c as a function of slab thickness Σa, in the J_2 and J_4 approximation

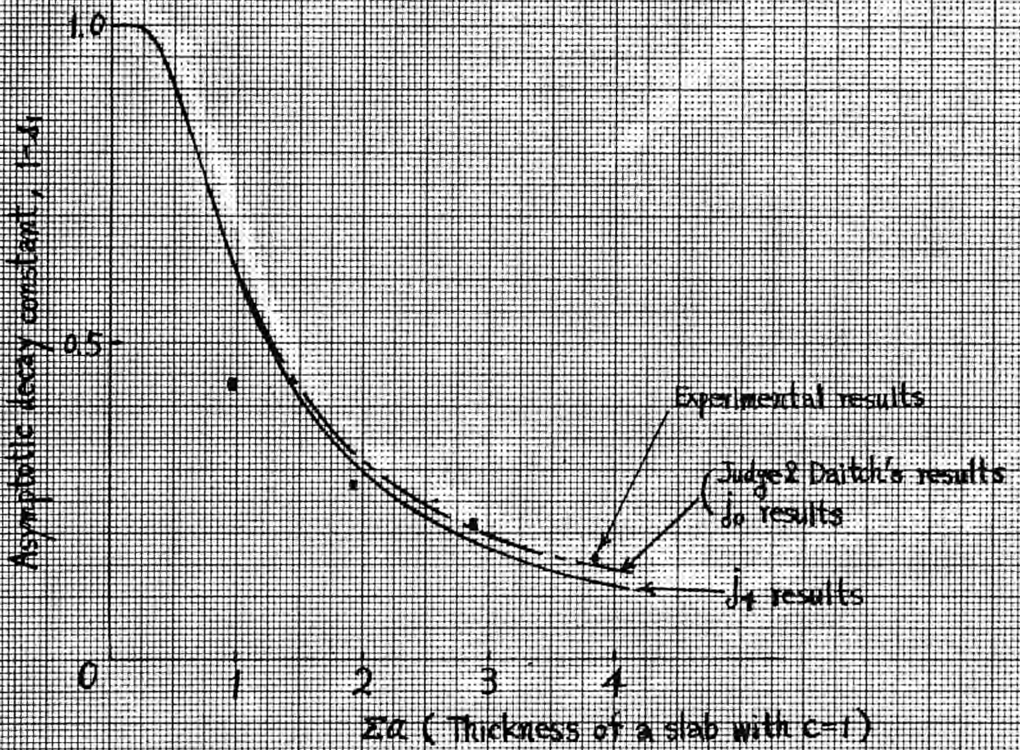

Fig. 15- Comparison of the asymptotic decay constant obtained from the j_0 or j_4 approximation with Judge & Daitch's calculated result and Beghian & Wilensky's experimental values

NOTICE TO THE READER

All Euratom reports are announced, as and when they are issued, in the monthly periodical **EURATOM INFORMATION,** edited by the Centre for Information and Documentation (CID). For subscription (1 year : US$ 15, £ 5.7) or free specimen copies please write to **:**

Handelsblatt GmbH
"Euratom Information"
Postfach 1102
D-4 Düsseldorf (Germany)

or

Office central de vente des publications
des Communautés européennes
2, Place de Metz
Luxembourg

To disseminate knowledge is to disseminate prosperity — I mean general prosperity and not individual riches — and with prosperity disappears the greater part of the evil which is our heritage from darker times.

Alfred Nobel

SALES OFFICES

All Euratom reports are on sale at the offices listed below, at the prices given on the back of the front cover (when ordering, specify clearly the EUR number and the title of the report, which are shown on the front cover).

OFFICE CENTRAL DE VENTE DES PUBLICATIONS DES COMMUNAUTES EUROPEENNES
2, place de Metz, Luxembourg (Compte chèque postal N° 191-90)

BELGIQUE — BELGIË
MONITEUR BELGE
40-42, rue de Louvain - Bruxelles
BELGISCH STAATSBLAD
Leuvenseweg 40-42, - Brussel

DEUTSCHLAND
BUNDESANZEIGER
Postfach - Köln 1

FRANCE
SERVICE DE VENTE EN FRANCE DES PUBLICATIONS DES COMMUNAUTES EUROPEENNES
26, rue Desaix - Paris 15e

ITALIA
LIBRERIA DELLO STATO
Piazza G. Verdi, 10 - Roma

LUXEMBOURG
OFFICE CENTRAL DE VENTE DES PUBLICATIONS DES COMMUNAUTES EUROPEENNES
9, rue Goethe - Luxembourg

NEDERLAND
STAATSDRUKKERIJ
Christoffel Plantijnstraat - Den Haag

UNITED KINGDOM
H. M. STATIONERY OFFICE
P. O. Box 569 - London S.E.1

EURATOM — C.I.D.
51-53, rue Belliard
Bruxelles (Belgique)